Modal Dynamics and Flutter Analysis of Floating Offshore Vertical Axis Wind Turbines

Faraz Ahsan [a], D. Todd Griffith [a,*], Ju Gao [a]

[a] *Department of Mechanical Engineering, University of Texas at Dallas, Richardson, TX, 75080, USA*

Abstract

Floating platforms provide vertical axis wind turbines (VAWTs) significant advantages over offshore horizontal axis wind turbines, which has led to increased research interest in offshore VAWT technology. This paper examines dynamic stability of floating VAWTs and presents structural dynamic and aero-elastic flutter analysis of utility-scale 5MW floating VAWTs by coupling a rotor finite element model with a linearized model for the floating system. The coupled floating VAWT model is utilized to study the effects of tower height, number of blades, blade tapering scheme, and impacts of the floating platform on modal properties and flutter. The study provides important new results and guidance to floating VAWT designers: (1) tower height increase leads to lower tower frequencies more prone to resonance, (2) by moving from land-based foundations to a floating TLP foundation, tower-mode frequency is increased significantly (by 49%-68%) which mitigates resonance and increases the flutter RPM (154% increase), (3) increasing the number of blades reduces the tower mode frequencies for both land-based and floating configuration, and (4) blade chord tapering can have a significant impact on increasing the tower mode flutter RPM. Further, analysis of low-frequency rigid body modes shows a safe, higher flutter RPM relative to the operating RPM.

Keywords:

Floating VAWT, Flutter, Structural Dynamics, Modal Analysis, Tapered Blades

1. Introduction

Research on offshore wind energy has shown an upward trend due to the availability of a better and more consistent wind resource. In an offshore context, VAWTs (vertical axis wind turbines)

*Corresponding Author. Email: tgriffith@utdallas.edu.

require smaller, cheaper floating platforms compared to that needed for HAWTs (horizontal axis wind turbines) [1, 2]. This is illustrated in Figure 1, where for HAWTs the drivetrain and generator are placed high above the water, a huge overturning moment is created that the floating platform has to stabilize, typically by adding mass to the substructure. This issue is less critical for offshore VAWTs because heavier components are placed closer to the water level. VAWTs are also less sensitive to wind veer compared to HAWTs. According to Quest Floating Wind Energy [3], VAWTs could help overcome wake effects that HAWT-based wind farms encounter. Also, VAWT blades can have less weight per length than HAWT blades since they are connected to the tower at both ends. Potential disadvantages of VAWTs include the decrease of aerodynamic efficiency due to the addition of struts that are required to maintain structural stability. Guy wires, which have been used in land-based VAWTs, could be challenging to incorporate offshore. However, a recent Sandia National Laboratories report estimates that due to less component cost, operation, and maintenance cost, offshore VAWTs could have a 25% decrease in cost of operation over a HAWT with the same capacity [4]. Harvesting maximum output from offshore VAWTs requires an adequate assessment of modal and flutter characteristics so that instability issues can be tackled, which is the focus of the current study to address this key issue that has not been adequately addressed for floating VAWT systems.

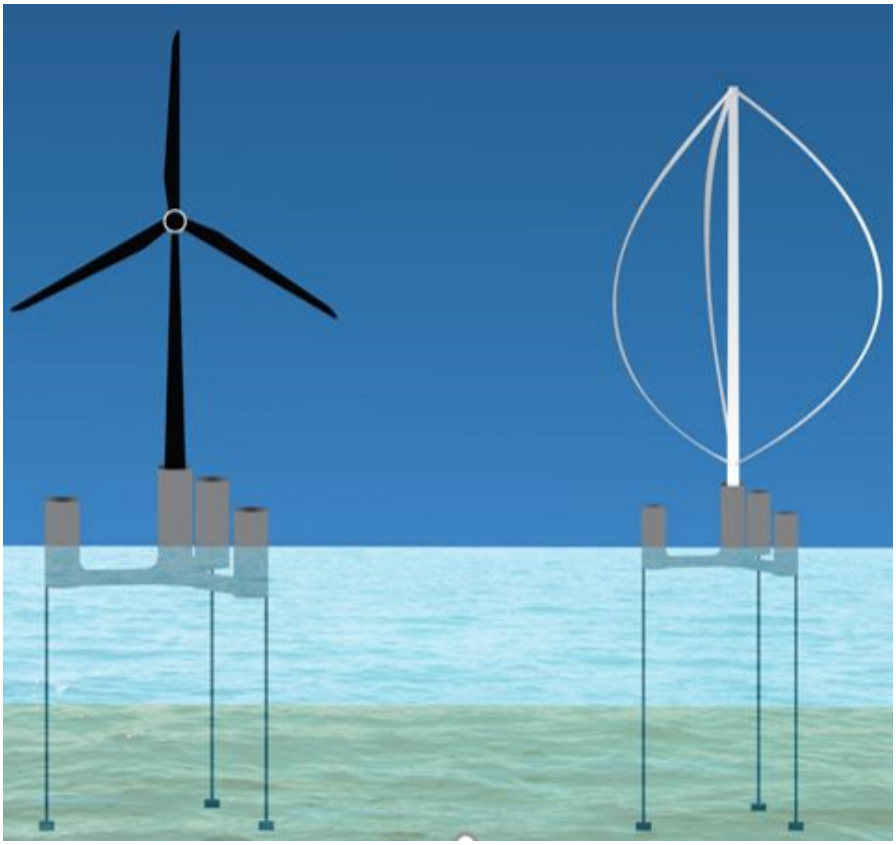

Figure 1: Comparing offshore HAWT and VAWT

Aero-elastic loads can initiate instability in structures that generate lift. For example, in HAWTs classical flutter is an aero-elastic instability that typically involves the coupling of first torsional mode and flapwise mode. At the early stage of flutter instability, the flapwise bending of blades creates Coriolis effect, which amplifies the torsional mode. The amplified torsional mode causes elastic deformation, which changes the aeroelastic forces and add more energy to the vibration modes. With HAWTs and VAWTs both being rotating, lift-generating structures, understanding the basics of flutter behavior in HAWTs could help address the flutter issue in VAWTs as well. The flutter phenomenon in large HAWT blades has been studied to obtain key insights. Lobitz [5] implemented classical Theodorsen's unsteady aerodynamic theory to analyze flutter characteristics of an isolated cantilevered wind turbine blade rotating in still air. Hansen [6] discussed stall induced vibration and classical flutter in HAWT blades and stated that attached flow, high tip speed, and low stiffness properties are some of the reasons for the flutter phenomenon. Another study [7] shows that increasing the size of the blade could initiate flutter instability in HAWTs since the long and slender nature of

larger blades make them prone to instabilities, thus this raises concern over possible flutter instability of large multi-megawatt offshore VAWT structures as well.

We now turn our attention to prior studies of structural dynamics and aero-elastic stability of VAWTs, where prior work focused on land-based deployments. The effectiveness of VAWTDyn and the commercial NASTRAN finite element (FE) software to predict resonance characteristics of the DOE/Alcoa 17-meter VAWT was studied by Lobitz [8], and it was observed that the FE modeling could better replicate the experimental results. Sullivan [9] summarized the initial modeling and experimental work on a VAWT at Sandia National Laboratories and pointed out that future studies on VAWT instabilities should include forced vibration analysis, revised rotor geometries and proper usage of hinges and pins. Popelka [10] employed NASTRAN to conduct flutter analysis for the Sandia 2-meter VAWT test-bed. Finite element modeling was experimentally validated using the data obtained for the Sandia 2-meter VAWT test-bed in the range of operating conditions. The study showed that flutter occurred due to coupling between the first flatwise bending vibration mode and the first torsional vibration mode. It was also observed that the flutter does not necessarily occur at the resonance frequency; it can be triggered when they have a close flatwise frequency.

Moreover, the torsional stiffness of tower and drivetrain significantly affected the torsional frequency and flutter speed. The flutter frequency was observed to be very close to the flapwise mode frequency. Finally, the experimental result showed that wind velocity reduces the rotational flutter speed (i.e., the flutter RPM), but its effect is negligible for operational wind speed. Carne et al. [11] compared the experimental modal analysis data of the Sandia 2-meter VAWT with the numerical results obtained from NASTRAN FE software. Although the agreement between these two analyses was not good at higher frequencies the average error was only 2.2 %, which was encouraging. Lobitz et al. [12] conducted a flutter analysis for the Sandia 34-meter test-bed, and it was concluded that tower and blade flutter RPM could be increased by adding a small amount of structural damping. Griffith et al. [13] conducted a modal analysis using step relaxation, random human excitation, and wind excitation to determine the first tower bending vibration mode of a 60 kW VAWT. Otterno [14] captured the eigenmodes of a three-bladed H-rotor and found that a large resonance-free RPM zone can be obtained by properly dimensioning the turbine. The aerodynamic damping of these eigen-

modes was observed to be good for wide and airfoil-shaped struts. The results showed that wind excitation provided the best estimates for frequency, damping, and mode shapes. Modal testing of small-scale VAWTs was performed by Kusnick [15] for a range of azimuth angles and three different extended tower heights. There was a substantial downward shift in resonant frequencies for extended tower heights, while azimuth position did not significantly affect resonance. The DeepWind [16] project analyzed a 5 MW VAWT through aeroelastic modeling framework of HAWC2, which employed the Actuator Cylinder [17] aerodynamics model for VAWTs. In the DeepWind study, the blade edgewise instability was observed over a range of operating conditions due to insufficient blade stiffness. The use of a stereo vision system for modal analysis on a parked three-bladed 1-kW VAWT was studied by Najafi [18]. The study showed that the stereo vision results and HAWC2 simulation agree within 4% for most vibration modes. Malcolm [19] performed a comparative study on the resonance issue of modified two- and three-bladed SNL 34-meter VAWTs. The analysis concluded that the rotors with three blades will encounter less critical resonance crossings than their two-bladed counterpart due to their axial symmetry associate with three-bladed turbines.

Owens et al. [20] addressed the modeling limitations associated with NASTRAN software by developing a new finite element-based structural model for HAWT flutter analysis. It was shown that the representation of complex-valued Theodorsen's function needs modifications to forecast the precise flutter margin of large blades. A coupled method to model the dynamic behavior of a floating VAWT was developed by Wang et al. [21] that was able to combine the hydrodynamics, wind flow, aerodynamics, structural dynamics and a generator control unit. Analysis in this model is performed in time domain to capture the interaction between the rotor, platform and mooring system. Hand et al. [22] studied the development of a cascade based computational model to achieve best balance between computational efficiency and accurate performance representation for a floating VAWT. Borg et al. [23] compared the feasibility of floating support structures between HAWTs and VAWTs. It was concluded that although the support structures that are used for floating HAWTs can also adequately support the floating VAWTs, the mooring system needed redesigning to restrain the surge, sway and yaw motion of the floating VAWT. Anagnostopoulou et al. [24] studied the dynamic performance of a floating VAWT on a 3-column semi-submersible and a 4-column semi-

submersible,and concluded that a 4-column semi-submersible is more suitable to meet the design weight and natural frequency of the system. Gao et al. [25] developed a 7-DOF model that takes into account aerodynamic, hydrodynamic and mooring loads to predict dynamic performance of a floating VAWT supported by tension leg platforms. The developed model compared two newly designed two-bladed and three-bladed floating VAWTs, and rendered the three-bladed VAWT better in terms of structural dynamics, power performance and fatigue life. Owens [26] developed an aeroelastic design framework called The Offshore Wind Energy Simulation (OWENS) for modeling large offshore VAWT rotor configurations. OWENS was developed with modular features such that aerodynamic, hydrodynamic, and drivetrain/generator modules can be interfaced to the core OWENS rotor structural model to perform transient modal analysis and flutter analysis of a wide variety of offshore VAWT configurations. Dynamic aeroelastic stability analysis was carried out [27] for six different Darrieus and V-type VAWT composed of glass and carbon material. It was observed in this study that the increased stiffness to mass ratio of carbon composite material better alleviates flutter concerns relative to heavier glass composite materials. Also, it was observed that the classical coupled flap-torsion flutter might not occur for VAWTS; however, instabilities involving only one mode could still be an issue for VAWTs. An initial study in Owens [28] to investigate the effect of monopile support and floating platform on the stability of offshore VAWT was performed to address the resonance concern. The monopile support condition was found to exacerbate the resonance concern while floating platform provided a better cushion against resonance.

This paper presents a comprehensive stability analysis for a multi-megawatt floating VAWT system, which we refer to as the UTD 5MW floating VAWT. In this work, we examine both structural dynamic performance as well as aero-elastic stability (or flutter) behavior. We begin this study with a comprehensive validation study of our VAWT structural dynamics and VAWT aero-elastic stability models. Although VAWT structural dynamics models have been validated in prior works, to the authors' knowledge this is the first study to perform validation of VAWT flutter predictions against numerical models and against experimental data. The validation studies demonstrate a very high level of agreement between our model and prior numerical and experimental results for both structural dynamics and aero-elastic stability (flutter) analyses.

Once the VAWT structural dynamics and flutter models are validated, we proceed to apply the models in a series of design studies for multi-megawatt floating VAWTs. In the first study, we examine both two-bladed and three-bladed configurations for the UTD 5MW VAWT for various tower heights above the mean water level. In a second study, the influence of four types of blade chord tapering is examined in the aero-elastic stability analysis. Then, we study the impact of the floating platform on the modes and frequencies of the floating VAWT system.

To summarize, the focus of this study includes identification of dominant VAWT flutter mode characteristics; addition of modeling capability of a floating platform into the OWENS code; study on the effect of tower height, blade number and blade tapering scheme on modal and flutter behavior of a VAWT. Additionally, this paper presents a first study of aero-elastic stability of a VAWT when placed offshore on a floating system where we examine the flutter potential of not only traditional flexible modes of the VAWT rotor, but also consider potential for flutter instability in the low-frequency rigid body modes of the floating system.

2. Structural Dynamic Modeling of Floating VAWTs

In this section, we discuss the modeling and analysis for the VAWT rotor and floating system. In order to analyze the VAWT rotor on a floating system, a structural dynamic model for the floating platform and mooring system must be coupled to the VAWT rotor model.

2.1. VAWT Rotor Structural Dynamic Modeling

OWENS [26] is a FEM-based toolkit developed by Sandia National Laboratories with capabilities of performing modal, flutter, and transient analyses for land-based VAWTs. The modularity of OWENS toolkit allows the coupling of the core OWENS rotor structural dynamics analysis tool with hydrodynamic, aerodynamic, generator and controller modules. VAWTGen [26] is a pre-processor to OWENS that generates the VAWT rotor geometry, FE mesh and other property files, with ability to model arbitrary VAWT configurations (Figure 2). The VAWT structure is discretized into a finite number of Timoshenko beam elements. Furthermore, VAWTGen can visualize the modal and transient results output by the OWENS analysis tool.

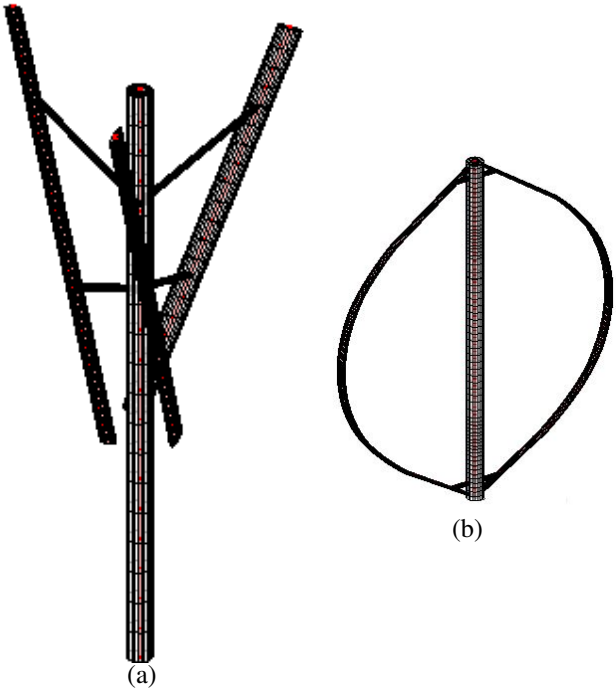

Figure 2: VAWTGen visualization (a) H VAWT, (b) Darreius VAWT

2.2. Coupled Floating VAWT Modeling

In this section, the modeling of the floating system and its coupling to the OWENS model is discussed. Via its modular interface, OWENS can couple with a user-defined floating system model. We approach this by modeling the platform as a 6DOF (degree of freedom) rigid body and the turbine as a rotating deformable-body in its native OWENS beam finite element formulation. Platform motion is defined in a fixed (non-rotating) coordinate system while turbine motion consists of deformation and rigid rotor rotation, and the motion of each node on the FEM mesh can be described as a combination of platform motion and turbine motion. The floating platform is modeled at the bottom of the tower as a 6DOF rigid body with the mass/inertia coupled to the node at the base of the tower and stiffness properties are modeled to account for hydrostatic restoring effects and mooring effects. The floating system consists of the platform and mooring, with hydrodynamic terms that can be modeled as frequency-dependent terms, in general.

The mass and stiffness properties are implemented based on a linearized structural dynamics model of the floating system, which is verified by a match of the six rigid body mode frequencies of the fully integrated VAWT rotor on the floating system to properly capture the system dynamics.

Viscous damping effects are also included to ensure the free-decay response captures the designed floating system behavior. Thus, with the addition of this 6DOF model for the mass, damping, and stiffness properties of the floating platform and mooring system we are able to perform structural dynamic analysis and flutter analysis of the integrated floating VAWT system.

In OWENS, the modal analysis of the entire floating VAWT configuration is performed on an equilibrium solution from a nonlinear static analysis including the rotational effects at various analyzed rotor speeds (RPM). Again, the floating platform is represented in a non-rotating frame, and modal and flutter analysis are performed in a co-rotating frame affixed to the rotating VAWT. The absolute deformation of each node of the system was analyzed by a combination of rigid displacement and flexible deformation, as described in Reference [26]. In FEM analysis, the equation of motion of the turbine only configuration is represented as:

$$M_V\ddot{x} + (C_V + G(\Omega))\dot{x} + (K_V(x) - S(\Omega))x = F_{cent}(\Omega) + F_{np} \tag{1}$$

Here, M_V, C_V, K_V are mass, damping and stiffness matrices of the turbine and x is generalized degree of freedom. $G(\Omega)$ and $S(\Omega)$ represent Coriolis matrix and spin-softening matrix at a rotor speed of Ω. F_{cent} is centrifugal force vector and F_{np} is a vector for non-potential forces such as aerodynamic force. Modal analysis is performed by solving equation (1) at different operating speeds (Ω).

Theodorsen unsteady aerodynamic theory is implemented to introduce aerodynamic loads for the flutter analysis. According to this theory, the lift and moment in terms of flapping and twisting motion of a cross-section is given as:

$$L = \pi\rho_\alpha b^2[\ddot{\omega} + V\dot{\theta} - ba\ddot{\theta}] + 2\pi\rho_\alpha VbC(k)[\dot{\omega} + V\theta + b(\frac{1}{2} - a)\dot{\theta}] \tag{2}$$

$$M = \pi\rho_\alpha b^2[ba\ddot{\omega} - Vb(\frac{1}{2} - a)\dot{\theta} - b^2(\frac{1}{8} + a^2)\ddot{\theta}] + 2\pi\rho_\alpha Vb^2(a + \frac{1}{2})C(k)[\dot{\omega} + V\theta + b(\frac{1}{2} - a)\dot{\theta}] \tag{3}$$

where b is semi-chord of an airfoil section, a is location of the elastic axis in fraction of semi-

chord, V is freestream velocity over the airfoil section, ρ_α is air density. $w(t)$ and $\theta(t)$ denote flapwise and torsional motion respectively. The complex valued Theodorsen function $C(k)$ models the amplitude and phase lag of aerodynamic forces acting on the airfoil section.

$$C(k) = F(k) + iG(k) \tag{4}$$

Here, $F(k)$ and $G(k)$ are real and imaginary parts of Theodorsen function. The 'reduced frequency' $k = \frac{\omega b}{V}$ depends on the oscillatory motion of the airfoil section. For a rotating turbine, the freestream velocity V is modeled as a function of distance from the hub axis r such that

$$V(k) = r\Omega \tag{5}$$

The aerodynamic mass, damping and stiffness can be modeled into equation (1) such that the aeroelastic system of equation is given by

$$(M_V + M_A)\ddot{x} + [C_V + G(\Omega) + C_A(\Omega,k)]\dot{x} + [K_V(x) - S(\Omega) + K_A(\Omega,k)]x = F_{cent}(\Omega) + F_A(\Omega) \tag{6}$$

Here, M_A, C_A and K_A are the aerodynamic mass, damping and stiffness matrices respectively. The combined formulation of the structural and aerodynamic terms can be presented as:

$$M_T\ddot{x_T} + C_T\dot{x_T} + K_T x_T = F_T \tag{7}$$

Here, $M_T = M_V + M_A$, $C_T = C_V + G + C_A$, $K_T = K_V + S + K_A$, $F_T = F_{cent} + F_A$. The equation of motion of the floating system is expressed as:

$$M_{FS}\ddot{x_{FS}} + C_{FS}\dot{x_{FS}} + K_{FS}x_{FS} = F_{FS} \tag{8}$$

Here, M_{FS}, C_{FS}, K_{FS} are mass, damping and stiffness matrices of the floating system. The dimension of x_{FS} is 6×1, and M_{FS} contains both platform mass and hydrodynamic added mass. The combined turbine and platform configuration can be represented in the following partitioned

matrix form

$$\left[\begin{array}{c|c} M_T^{base}+M_{FS} & m \\ \hline m & M_T^* \end{array}\right]\ddot{x_T}+\left[\begin{array}{c|c} C_T^{base}+C_{FS} & c \\ \hline c & C_T^* \end{array}\right]\dot{x_T}+\left[\begin{array}{c|c} K_T^{base}+K_{FS} & k \\ \hline k & K_T^* \end{array}\right]x_T=\left[\begin{array}{c} F_T^{base}+F_{FS} \\ \hline F_T^* \end{array}\right] \quad (9)$$

Here, M_T^*, C_T^*, K_T^*, F_T^* are turbine model partitions containing all DOFs except for the 6 base node DOFs. M_T^{base}, C_T^{base}, K_T^{base} contain the base node DOF (6×6 partition) of turbine model. The floating system model terms M_{FS}, C_{FS}, K_{FS} and F_{FS} are added at the base node of the turbine. The terms inside partitioned matrices m, c, k are not zero. Following is the completed set of equation of motion of floating VAWT

$$M\ddot{x_T}+C\dot{x_T}+Kx_T=F \quad (10)$$

Here, M, C, K, F are combined mass, damping, stiffness and load matrices for the coupled floating VAWT system. Equation (10) represents a fully coupled dynamic model that combines rotor structural dynamics and floating platform dynamics. This equation takes into account the unsteady aerodynamic loads, and hence is capable of performing unsteady flutter analysis of the coupled rotor-platform system. Due to the addition of rigid platform to the turbine, the absolute displacement of each node in equation (10) is dependent on rigid body translation, rigid body rotation and flexible deformation such as:

$$\underline{x_T^i}=\underline{T}\,\underline{x_T^0}+\underline{u_T^i} \quad (11)$$

Here, $\underline{x_T^i}$ is absolute displacement vector of node i, $\underline{T}$ is the matrix taking into account the rigid body rotational terms, $\underline{x_T^0}$ is the rigid body rotation of the node where the rigid platform is modeled at, and $\underline{u_T^i}$ is flexible deformation of node i. In the final formulation of gyric and spin-softening matrices it was ensured that there was no gyric and spin-softening effect on the rigid body modes due to the rigid body modes while the cross-coupling of gyric and spin-softening terms between rigid modes and flexible modes were retained.

For modal analysis, the forcing terms are removed from equation (10) and the resulting 2^{nd} order aero-elastic equation is converted to 1^{st} order equation by state-space formulation to carry out the eigen analysis. The converted system of 1^{st} order equation can be stated as:

$$\overline{M}\dot{\underline{X}} = \overline{A}\underline{X} + f_o \tag{12}$$

Here, $\underline{X}$ is the vector that contains state variables of the system. This equation is assumed to have solution of the following form

$$\underline{X} = \underline{\phi} e^{\beta t} \tag{13}$$

which, when substituted into equation (12) gives the geenralized eigenvalue problem:

$$(\overline{A} - \beta\overline{M})\underline{\phi} = 0 \tag{14}$$

Now the flutter analysis procedure is summarized. The solution of this eigenvalue problem results in a set of eigenvalues β_j and corresponding eigenvectors $\underline{\phi_j}$. The imaginary part of every eigenvalue $Im(\beta_j)$ is frequency parameter and the real part $Re(\beta_j)$ is the stability parameter. A positive eigenvalue real part corresponds to a negatively damped system. In our analysis, the rotor RPM is varied, and positive eigenvalue real part (negative damping) is searched for. The rotor RPM at which a particular mode shows negative damping is stated as the flutter RPM of that mode of vibration.

3. Validation of VAWT Models for Structural Dynamics and Flutter

We begin the study by performing validation of both our structural dynamics and aero-elastic stability capabilities for VAWTs by comparing our simulations with prior numerical studies and with prior experimental studies. The capability of OWENS to accurately predict modal and flutter characteristics of land-based Sandia 34-meter and Sandia 2-meter VAWTs has been studied. For both turbines, a modal analysis was carried out in OWENS to compare parked rotor frequencies with the experimentally obtained values. Afterward, values of flutter RPM associated with tower

and blade vibration modes obtained from OWENS were compared with the experimental flutter data. Furthermore, our model was also validated with experimental flutter results considering the effect of additional structural damping.

3.1. Validation for the Sandia 34-meter Testbed

Experimental test data for the Sandia 34-meter (SNL34m) [12] VAWT was first used to validate the OWENS toolkit. Modal frequency and flutter RPM were calculated by OWENS, and the results are compared to experimentally obtained parked rotor frequencies and flutter RPM predictions. Table 8 shows that the first six modal frequencies obtained in this study for rotor are in good agreement with modal analysis results, and the maximum difference of 7.6% associated with the 1st Flatwise Antisymmetric mode frequency. It is worth mentioning that the tower vibration modes are not compared here since a pinned tower top and base tower base boundary conditions were employed for this guy-cable supported rotor, and thus the tower modes appear at higher frequencies. The pinned boundary condition allows the tower to rotate about its own vertical axis of rotation.

Mode	Modal test	Current study	% Difference
1st Flatwise Antisymmetric	1.06	0.98	-7.6
1st Flatwise Symmetric	1.06	0.99	-6.6
1st Propeller	1.52	1.59	4.6
1st Edgewise	1.81	1.68	-7.2
2nd Flatwise Antisymmetric	2.06	2.01	-2.4
2nd Flatwise Symmetric	2.16	2.04	-5.6

Table 1: Sandia 34m VAWT Parked Modes Comparison

Lobitz and Ashwill [12] analyzed the flutter characteristics for Sandia 34-meter VAWT for the cases of aerodynamic damping only and for a combination of aerodynamic and structural damping. This study showed that although a small additional structural damping stabilizes 1st tower and 1st butterfly modes, these two modes become unstable at relatively lower RPM than the 2nd Flatwise mode, and 2nd Flatwise mode is the dominant mode of flutter for this turbine. Here, the study conducted by Lobitz and Ashwill [12] was used for validation of the current flutter analysis. The present study indicates good agreement with Lobitz and Ashwill's finding, as shown in Table 2 and

Figure 3. According to the results while considering only the aerodynamic damping case, it was found that differences of 5.5% and 2.1% were observed for the predicted flutter speeds for the tower and 2nd flatwise mode flutter modes, respectively. This small discrepancy is likely because the concentrated mass (mass of bolts, nuts etc) elements were not exactly implemented in our model.

	Flutter rpm (Aerodynamic Damping Only)	
	Tower mode	2nd Flatwise mode
Lobitz	38	82
Current Study	40.1	83.7
% Difference	5.5	2.1

Table 2: Sandia 34m VAWT Flutter RPM Comparison

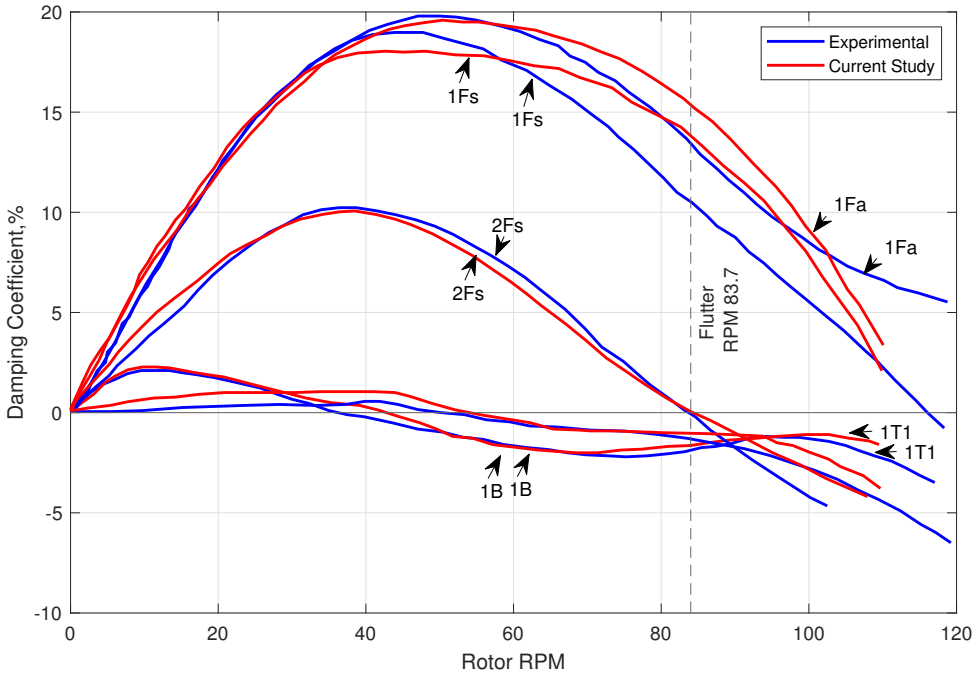

Figure 3: Damping coefficient versus RPM for the flutter analysis of the SNL 34-meter VAWT (Aerodynamic Damping Only)

Lobitz and Ashwill [12] also added 2% structural damping to demonstrate the effect of structural damping in the flutter prediction. They found that tower flutter mode could be delayed beyond the operating RPM, which makes the 2nd flatwise mode the dominant unstable mode. In the present

study, we also added 2% structural damping to our 34-meter VAWT model, and the results were similar to that of Lobitz and Ashwill [12], as compared in Table 3 and Figure 4 with 1.9% and 2.4% difference in prediction of tower and 2nd flatwise mode flutter speeds when 2% structural damping is added.

	Flutter rpm (Aerodynamic +2% Structural Damping Only)	
	Tower mode	2nd Flatwise mode
Lobitz	107	89
Current Study	109	91.1
% Difference	1.9	2.4

Table 3: Sandia 34-meter VAWT Flutter RPM Comparison (Aerodynamic Damping + 2% Structural Damping)

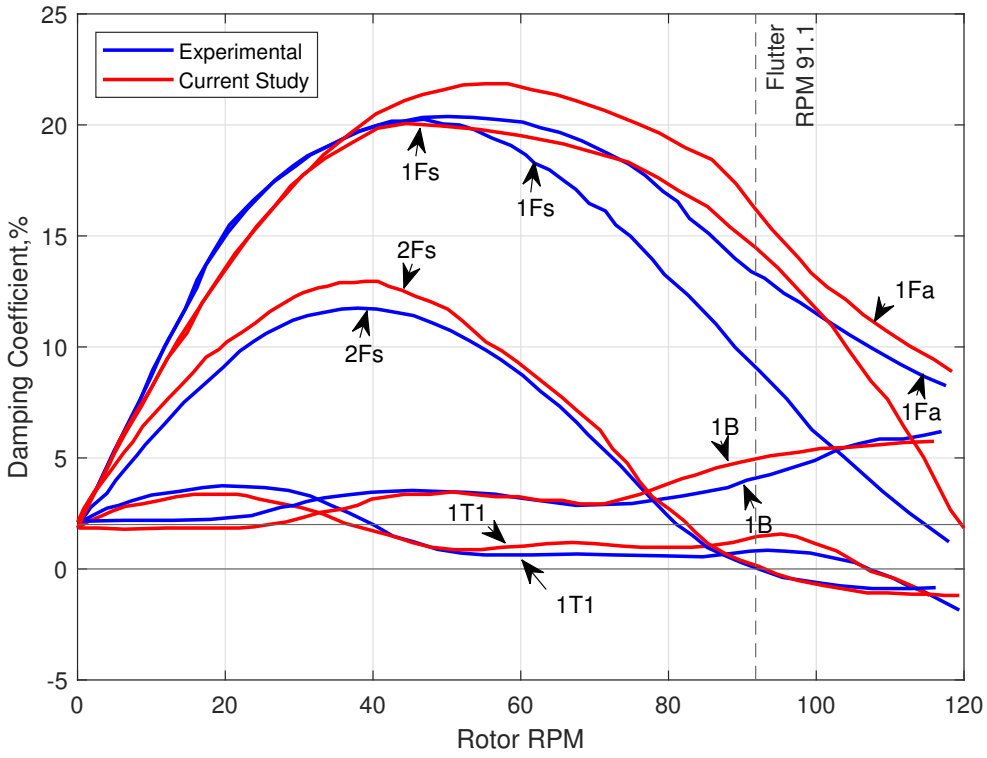

Figure 4: Damping coefficient versus RPM for the flutter analysis of the SNL 34-meter VAWT (Aerodynamic Damping + 2% Structural Damping)

3.2. Validation for the Sandia 2-meter VAWT

A second validation for modal and flutter models used here was performed for the Sandia 2-meter VAWT [10]. Parked modal frequencies and fan plot was published by Carne [11] for the Sandia 2-meter VAWT. The results obtained from the OWENS analysis show an acceptable agreement with experimental data [10] for the parked frequencies, as displayed in Table 4, and the fan plot is reported in Figure 5. Although the frequencies show some dissimilarities in the high RPM range for the higher modes, the trajectory of the modes indicates a good match.

Mode Number	Mode	Measured	Current study	% Difference
1	1st Antisymmetric Flatwise	12.3	11.58	-5.9
2	1st Symmetric Flatwise	12.5	11.82	-5.6
3	1st Rotor Out of Plane	15.3	14.5	-5.2
4	1st Rotor in Plane	15.8	15.0	-5.1
5	Dumbbell	24.4	22.58	-7.5
6	2nd Rotor Out of Plane	26.2	24.7	-5.7
7	2nd Rotor in Plane	28.3	28.45	0.5
8	2nd Symmetric Flatwise	29.7	31.15	4.9
9	2nd Antisymmetric Flatwise	31.5	33.12	4.9
10	3rd Rotor Out of Plane	36.5	34.42	-5.7

Table 4: Sandia 2-meter VAWT Parked Frequency Comparison

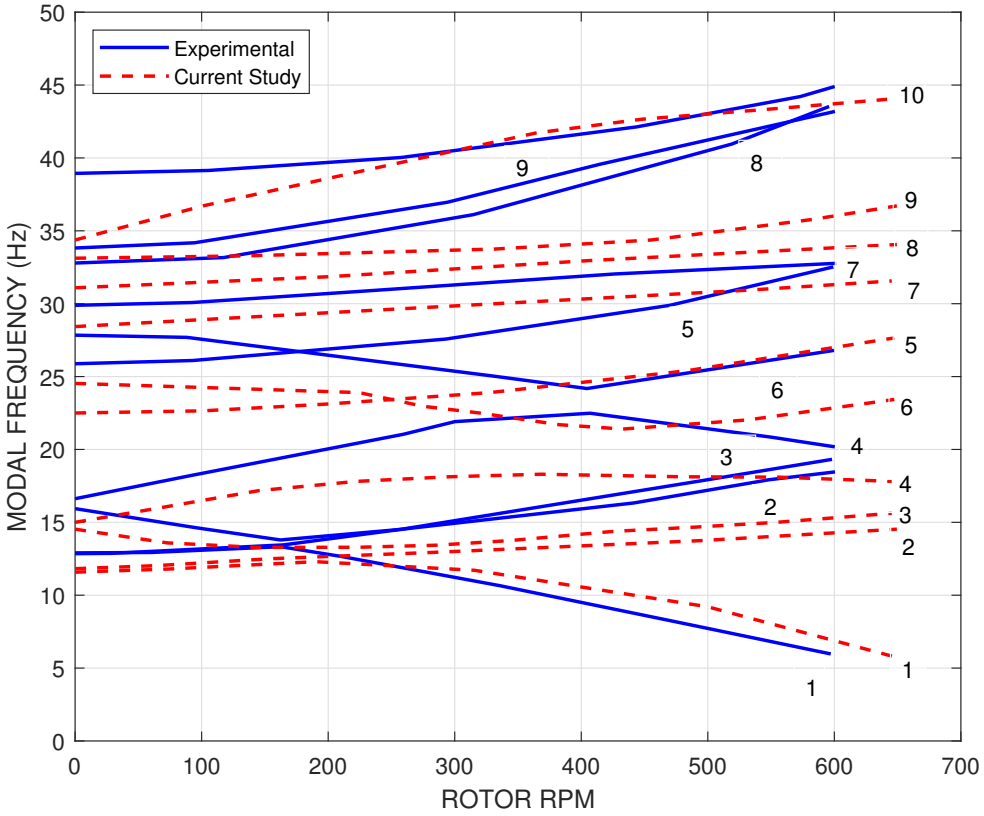

Figure 5: Sandia 2-meter VAWT Modal Frequency versus RPM (a) Experimental, (b) Current Study

Popelka [10] carried out experimental flutter analyses for the Sandia 2m VAWT. The OWENS toolkit was validated by analyzing the three-bladed Sandia 2m VAWT with NACA 0012 airfoil and a chord size of 2.91 inches. Using the model used for Table 4 and Figure 5, we now predict the flutter speeds for the Sandia 2-meter VAWT. Table 5 and Figure 6 show that there is a good agreement in predicting the flutter RPM of the flatwise mode of the land-based Sandia 2-meter VAWT.

	Experimental	Current study	% Difference
Flatwise RPM	745	801	6.99
Flatwise Frequency	18	18.92	5.1

Table 5: Sandia 2-meter VAWT Flutter RPM Comparison

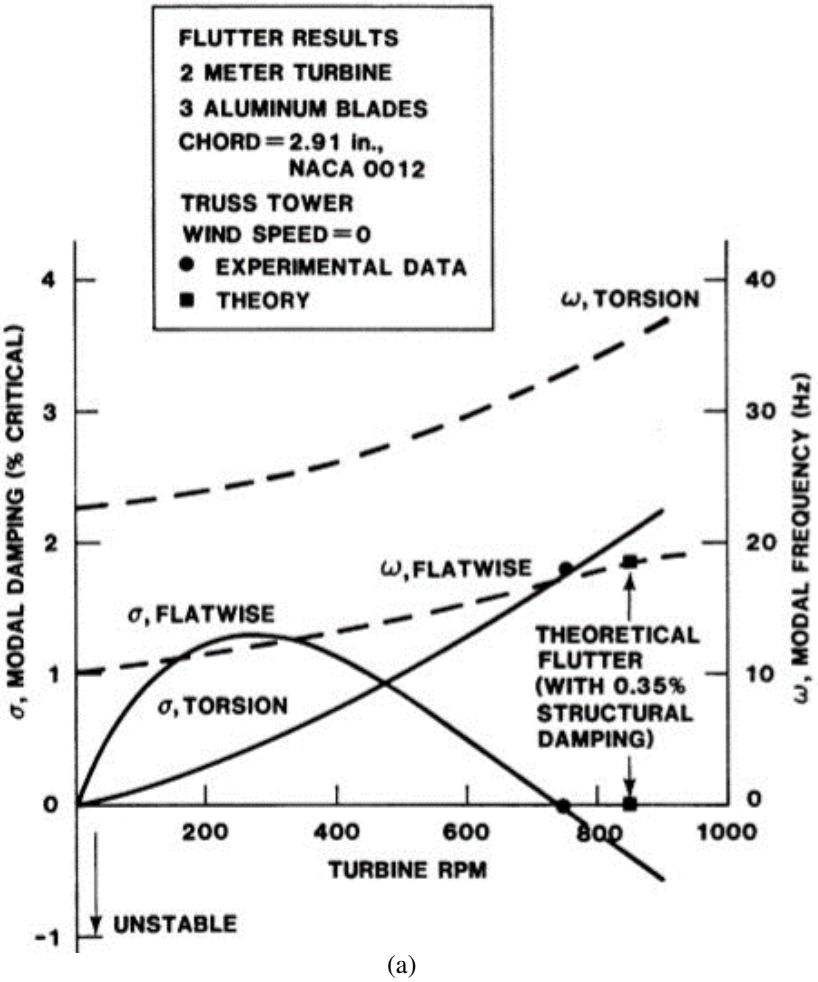

(a)

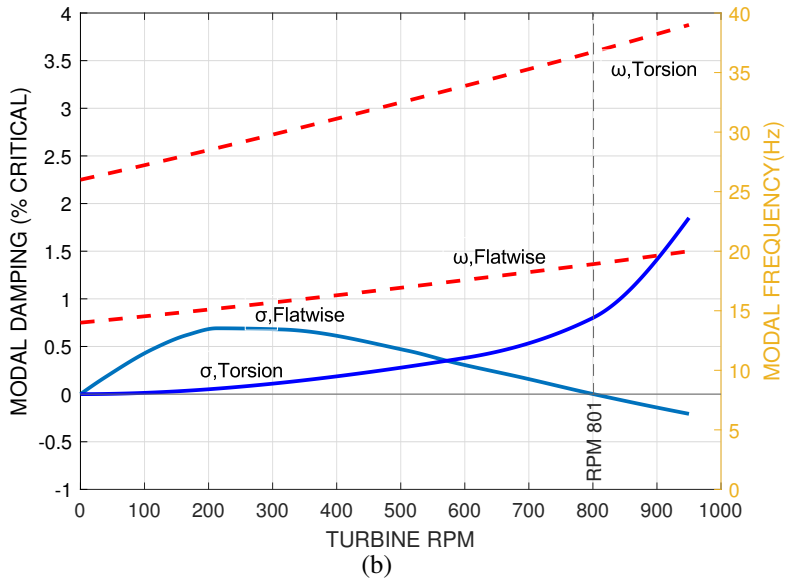

(b)

Figure 6: Sandia 2m VAWT Flutter Stability Analysis: (a)Experimental [10] , (b) Current Study

277 The capability of the present model to closely match the experimental data for the parked and

rotating Sandia 2-meter and Sandia 34-meter VAWTs was proved through validation for both modal analysis and flutter analysis predictions. Campbell diagrams generated by OWENS exhibit a trend very similar to the experimental fan plots, which indicates that the applied model can capture all the rotor rotational effects as well. In this section, the high accuracy of present model to identify the flutter modes was confirmed for both turbines.

4. UTD-5MW Offshore VAWT Specification

The current study primarily focuses on two-bladed and three-bladed offshore VAWTs on a tension leg platform with a power rating of 5MW. The turbine contains blades, struts and tower and operates at fixed rpm. The blade design software called NuMAD [29] provided the beam properties of the turbine, and VAWTgen produced surface render visualization for turbines, as shown in Figure 7. The input files to carry out structural dynamic analysis for this UTD-5MW VAWT [30] were generated by VAWTGen. Table 6 contains the structural properties of this turbine.

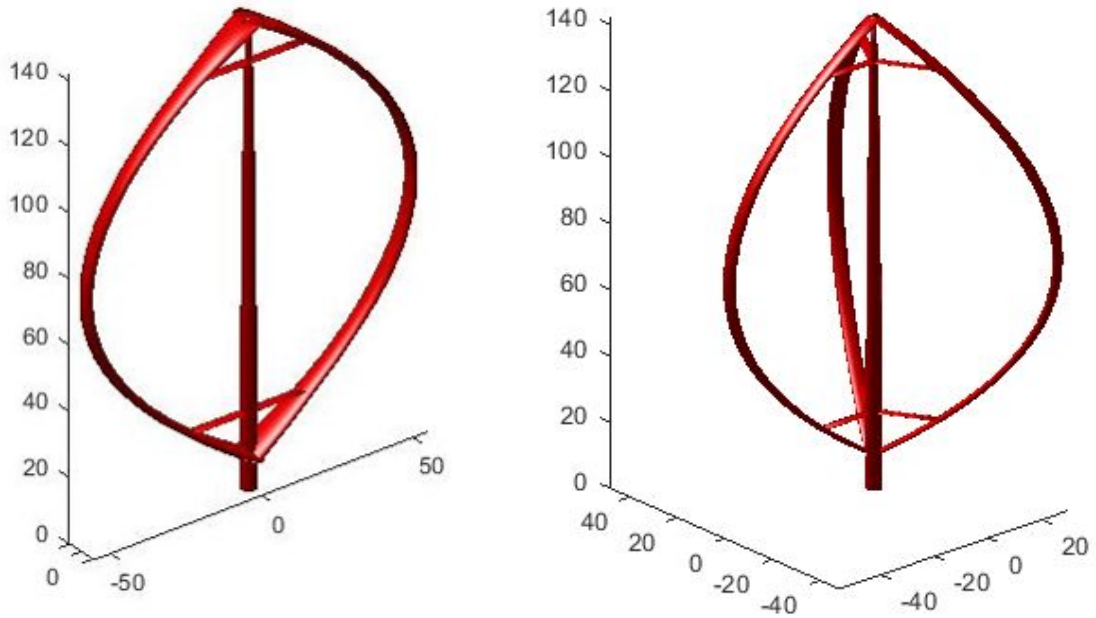

(a) (b)

Figure 7: UTD 5MW VAWTs: (a) Two-bladed, (b) Three-bladed

Design Version	VAWT 5MW 2B	VAWT 5MW 3B
Rotor Type	Darrieus	Darrieus
Number of Blades	2	3
Rated Power [MW]	5	5
Blade Height [m]	132.2	132.2
Tower Height [m]	142.2	142.2
Rotor Diameter [m]	108.2	108.2
Chord [m]	Varies from 6 to 3	Varies from 6 to 3
Blade Length [m]	177.1	177.1
Blade mass [Kg]	17,300	37,186
Blade CG [m]	76.0	77.7
Tower Mass [Kg]	175,000	175,000
Tower CG [m]	53.52	53.52
Rotor Mass [Kg]	220,480	322,250
Rotor CG [m]	57.97	64.35

Table 6: UTD 5MW VAWT Rotor Specification: Two-bladed (2B) and Three-bladed (3B) Designs.

Two initially designed TLP-type floaters which were developed from the TLP wind designs [31, 32] are applied as the supporting floaters for the two- and three-bladed rotors in deep water, respectively. The TLPs contain one center column where the tower is located and three outer columns connecting with the center column by three rectangular pontoons, respectively. Each outer column is connected with one mooring tendon which is always in tension. The motions of the TLPs especially the heave, roll, and pitch motions are limited by the tendons. Table 7 summarizes main properties of the two floating VAWTs. Figure 8 shows the configuration of the two-bladed floating VAWT used in this study. CoP in the figure represents the aerodynamic pressure center of the rotor, where wind loads are applied, and CoG represents the center of gravity of the TLP.

The frequency dependent radiation damping coefficient computed using a diffraction program is included in the calculation to represent the wave damping. Additional linear viscous damping force F_d is added to the floating VAWT system to accurately represent the physical system:

$$F_d = -C_d \dot{X} \tag{15}$$

where C_d represents the linear viscous damping coefficient, and $\dot{X}$ is the velocity of the platform.

	Unit	Floating VAWT (2B)	Floating VAWT (3B)
Water depth	m	100	100
Draft	m	15	15
Total mass (turbine+hull+ballast)	ton	1981	2148
Buoyancy in undisplaced position	ton	3302	3465
CoG above MWL	m	6.7	10.0
Radius of gyration about CoG: Roll	m	30.3	36.9
Radius of gyration about CoG: Pitch	m	30.3	36.9
Radius of gyration about CoG: Yaw	m	16.4	19.6
Mooring length	m	85	85

Table 7: Characteristics of two TLP-type floating VAWTs

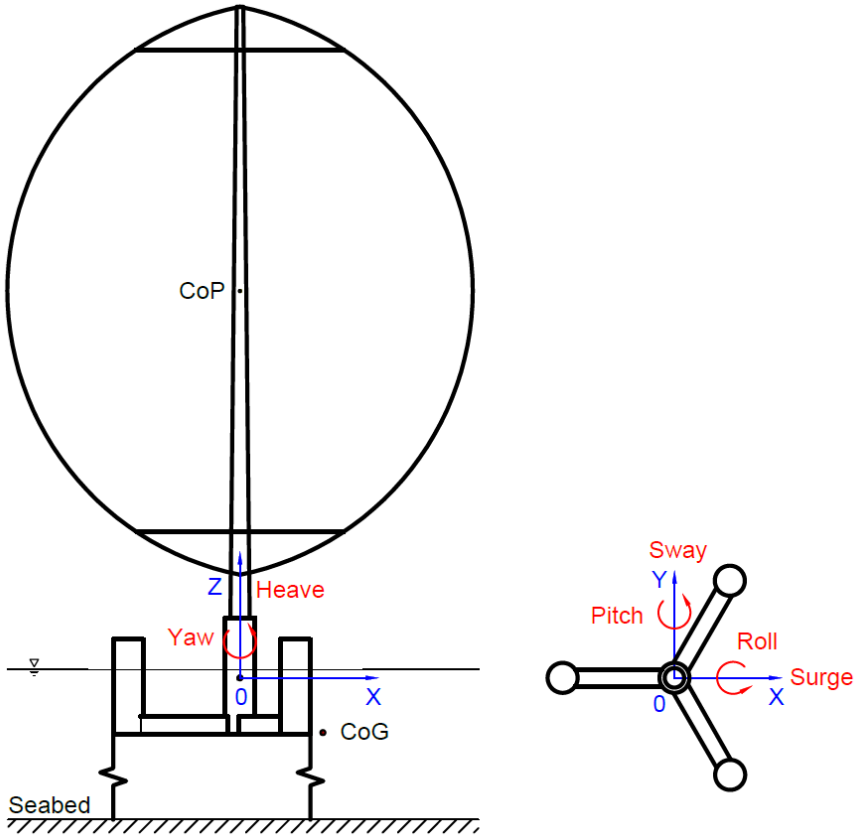

Figure 8: A two-bladed floating VAWT configuration and its 6-DOF coordinate system

5. Design Studies for the UTD 5MW VAWT

The first six flexible modes of the UTD 5 MW two-bladed VAWT were obtained from OWENS and are plotted in Figure 9. Vertical axis wind turbines have significantly different geometry than HAWTs. As a result, the mode types are quite distinct in VAWTs. Further, the classical flutter pattern for HAWTs that involves coupling between flap and torsion modes might not be observed in some VAWT configurations. However, the flutter prediction procedure employed here for the VAWT follows the classical approach used for HAWTs by performing modal analysis for the aero-elastic system for varying, increasing RPM until a flutter mode with negative damping is identified.

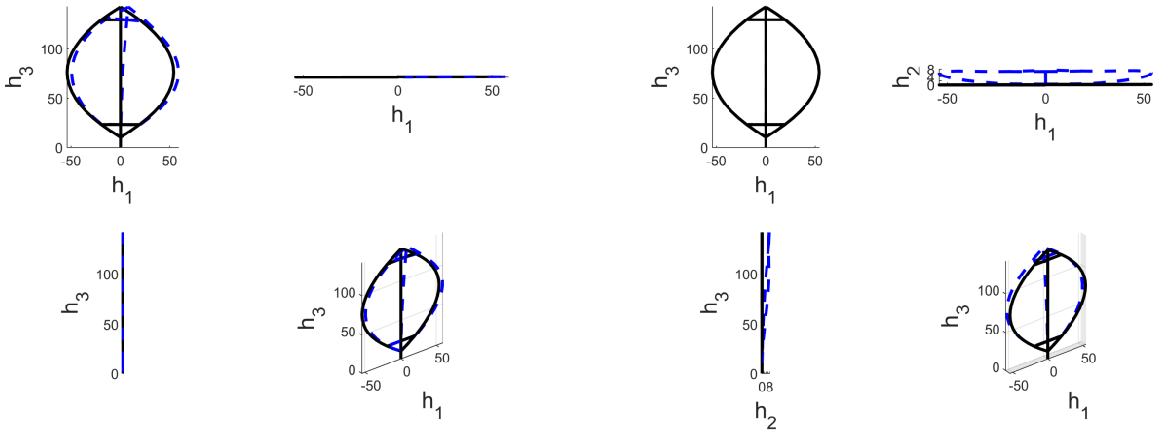

(a) In Plane Tower Mode (b) Out of Plane Tower Mode

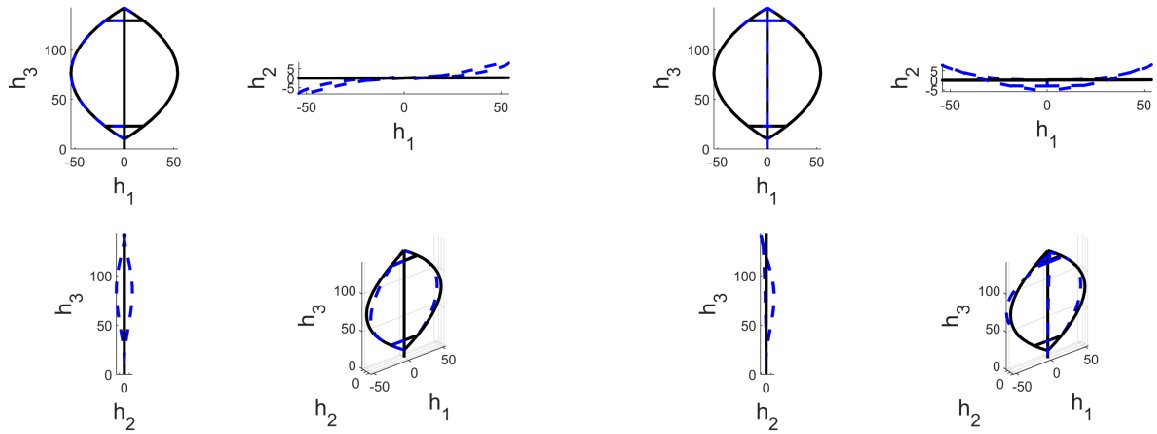

(c) Propeller Mode (d) Edgewise Mode

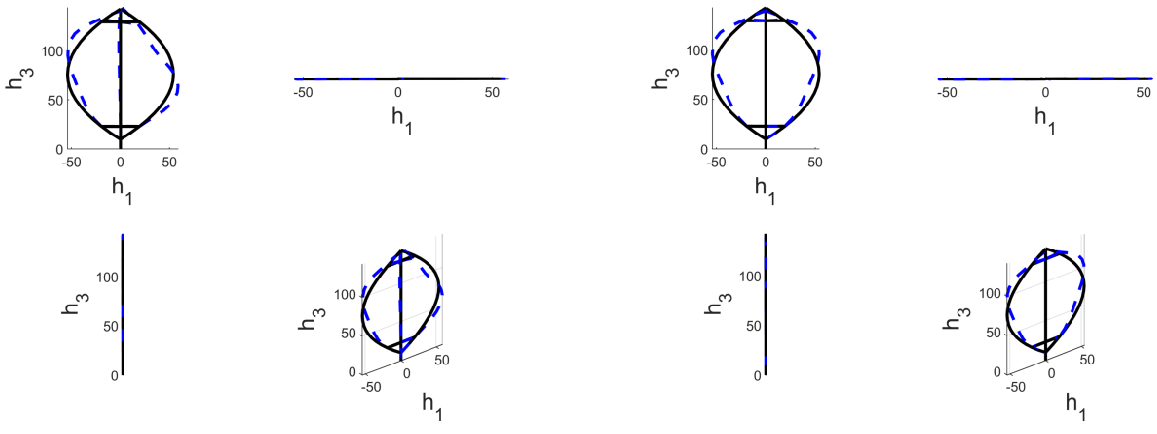

(e) Antisymmetric Flatwise Mode (f) Symmetric Flatwise Mode

Figure 9: First Six Flexible Modes for the Parked UTD 5MW Two-bladed Rotor

311 Based on the flutter analysis for the two turbines specified above (UTD 5MW VAWTs with two

and three blades), it was found that tower, propeller, and edgewise modes are the three primary flutter modes for UTD 5 MW VAWT. We note that these principal flutter modes deviate from the classical flap-torsion or edge-torsion coupling behavior. Figure 10 shows these three representative cases where the tower vibration mode shows up mostly in the in-plane and out-of-plane directions similar to the bending of a cantilever beam. For a two-bladed VAWT, the blades move simultaneously equal distance in a lead-lag fashion similar to the flapping wings of a butterfly when seen from above in edgewise mode. In propeller mode, the two blades move in phase in opposite direction where the vertical tower becomes the axis of rotation.

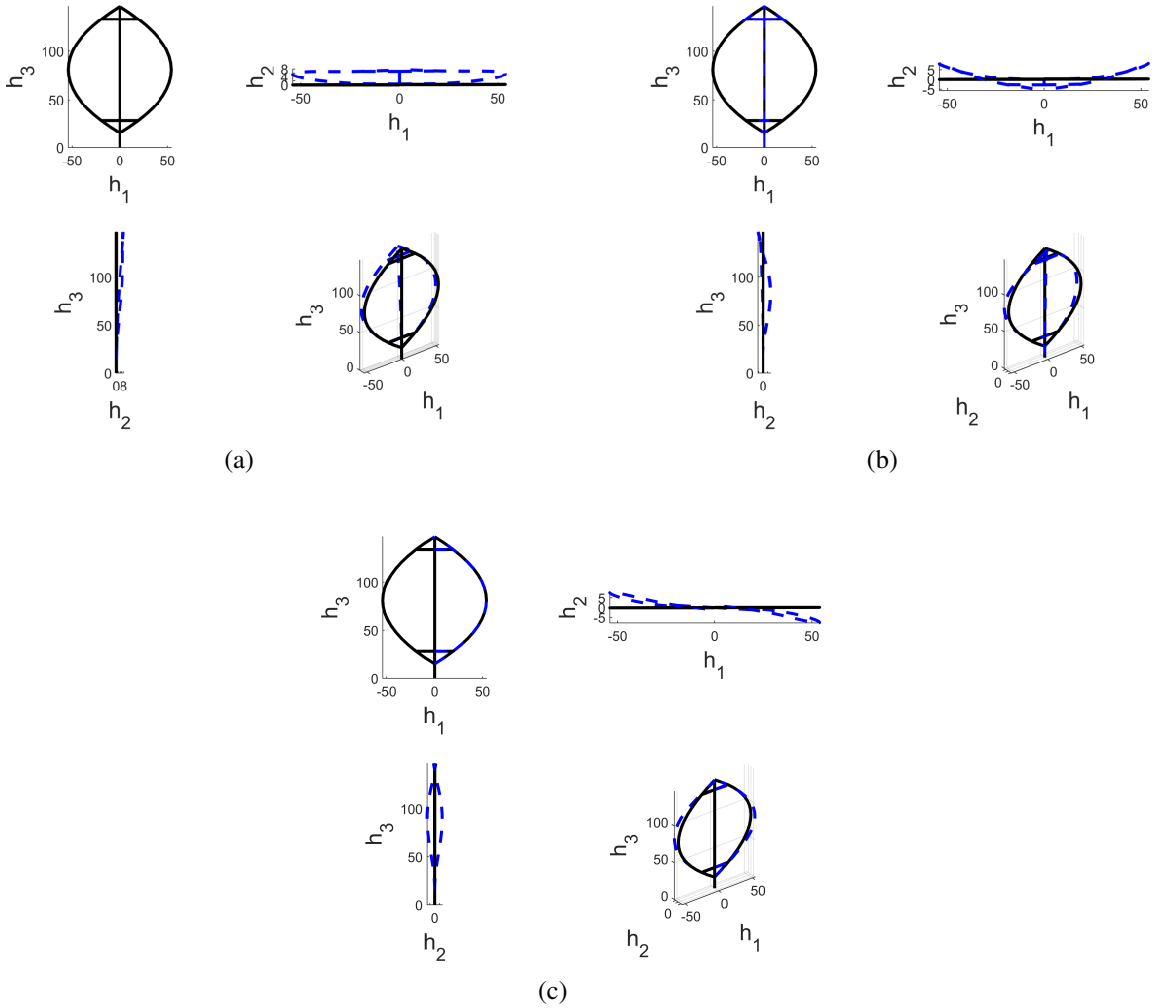

Figure 10: Visualization of the Flutter Modes (a) Tower Mode, (b) Edgewise Mode, (c) Propeller Mode

In this analysis, the tower mode shows hard flutter (see Figure 11(a)), and propeller/edgewise modes exhibit soft flutter (see Figure 11(b)). Soft flutter modes show a smooth transition from

positive to negative damping ratio, while hard flutter modes have a steep, sudden slope during this transition, as depicted in Figure 11(a). The values of damping ratio for hard flutter mode are considerably higher than soft flutter mode.

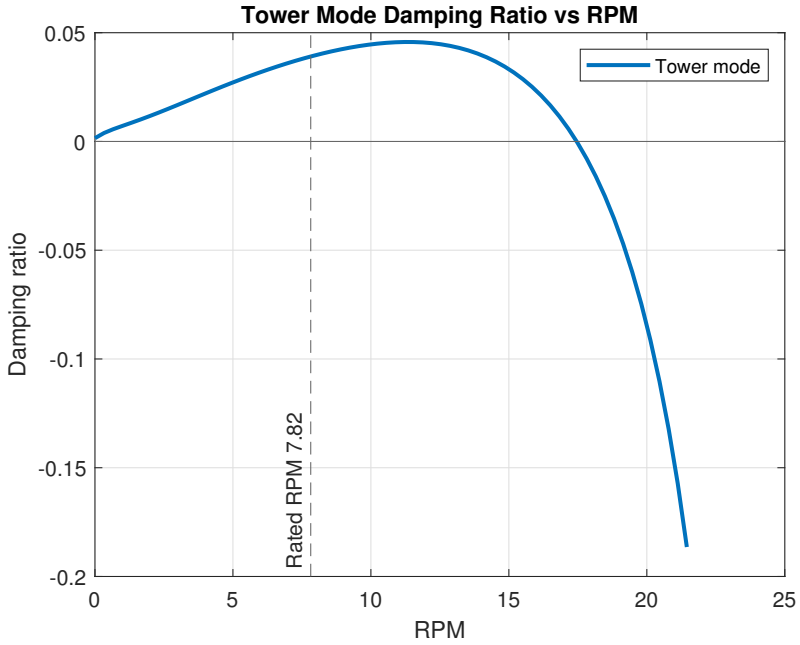

(a)

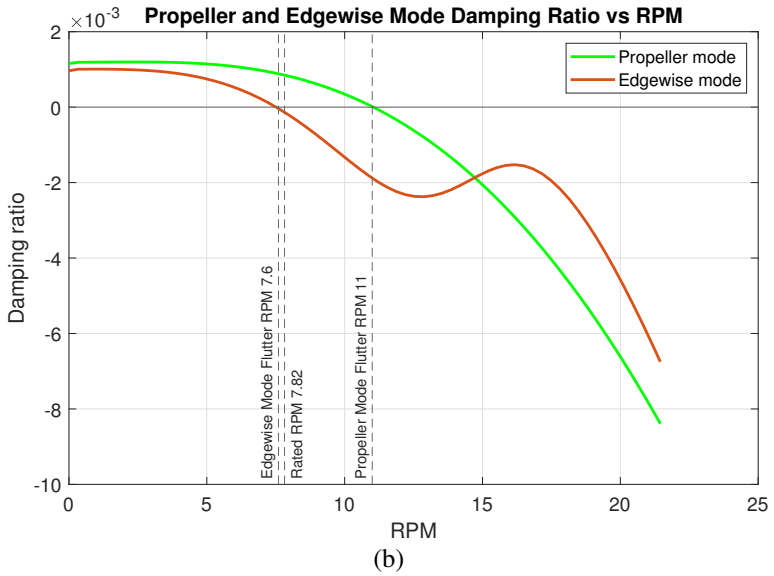

(b)

Figure 11: (a) Hard Tower Mode Flutter, (b) Soft Propeller and Edgewise Mode Flutter

The tower mode flutter is the primary design concern since the soft propeller/edgewise mode flutter RPM can be pushed beyond the operating RPM by adding minor structural damping to the VAWT system, and the tower mode exhibits a hard flutter, which has potential to be more catastrophic. To

show the effect of adding structural damping, the Rayleigh damping parameter was added to damp out lower frequency modes. Figure 12(b) shows that adding a 1% structural damping to the general damping increases the propeller and edgewise mode flutter from (no structural damping case) 4.9 and 3.3 RPM to 11 and 7.6 RPM, respectively. As shown in Figure 12(c), adding 2% damping ratio (as was done in [10] for the Sandia 34-meter VAWT) further delays the soft flutter modes' RPM, although it does not alter the hard tower mode flutter RPM much.

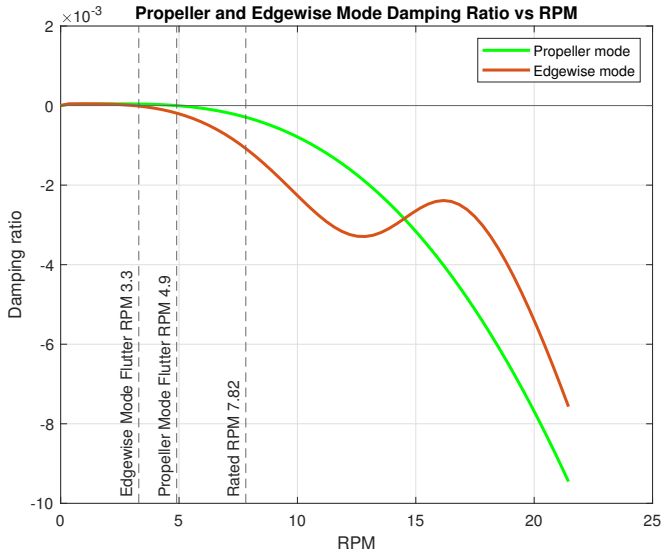

(a)

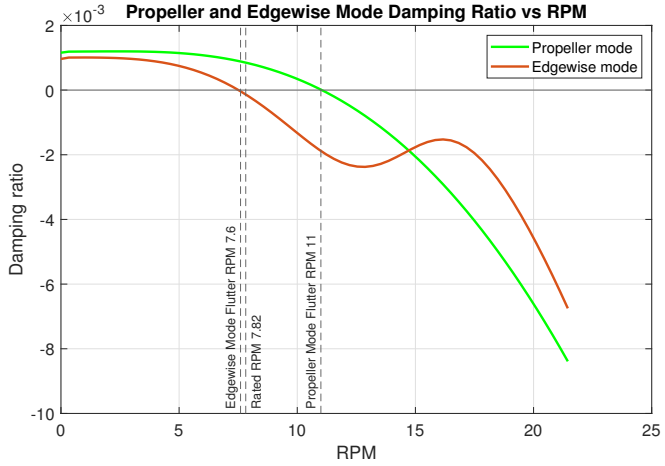

(b)

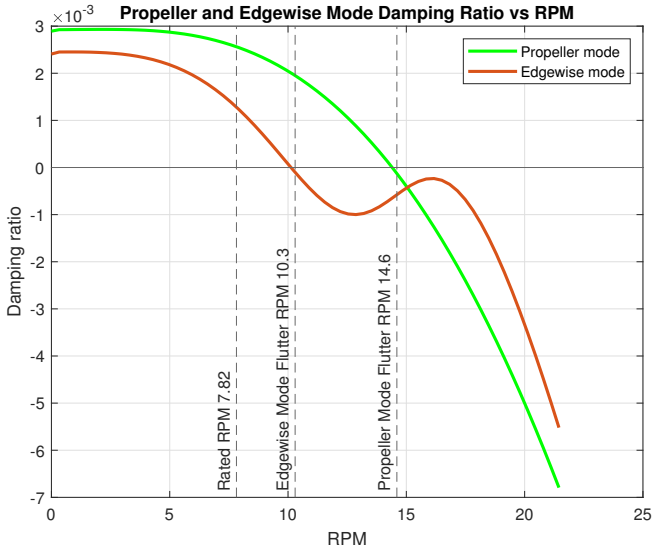

(c)

Figure 12: Soft flutter modes with (a) No Structural Damping, (b) 1% Structural Damping, (c)2% Structural Damping

In this initial study, we have identified and characterized the fundamental behavior of the modal and flutter characteristics of large-scale VAWT rotor as this was evaluated in this section. We now turn our attention to the impact of the important design requirements on modal and flutter performance, as the primary focus of this overall study, which is assessed through a study of various rotor and floating system design choices. For example, what impact does the tower height have on modes and flutter? How does tapering of the blade chord impact flutter speeds? And, what is the impact of the floating system on turbine modes and flutter speeds? These are some of the research questions addressed in the following sections through an aero-hydro-elastic parametric study.

5.1. Effect of Tower Height and Number of Blades on Flutter

Tower height could play a pivotal role in the resonance and stability concerns of offshore VAWTs; therefore, in this section we perform a study of the impact of tower height on VAWT structural dynamics and flutter. Figure 13 shows three tower height extensions of 10, 15, and 20 m that we consider. For each case, the tower height has been extended downward from the intersection of tower and blade root while adjusting the tower properties accordingly.

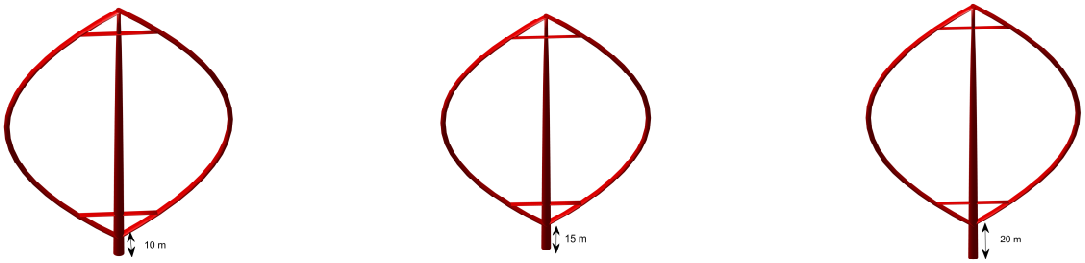

(a) (b) (c)

Figure 13: Tower Height Variation: (a) 10 m extension, (b)15m extension, (c) 20m extension

Typically, extending the tower height has a detrimental effect since this reduces the tower mode frequencies, and there could be crossings with the per-rev excitations of the rotor that depend on the number of blades. A flutter analysis was performed for the above range of tower heights, and the effect of tower height extension can be observed in Figure 14 for the three flutter modes of interest for two- and three-bladed VAWTs, which are the tower, propeller, and edgewise flutter modes. Extending the tower height reduces the tower mode flutter RPM since with the increase of tower

length, the stiffness to mass ratio of the configuration decreases. On the other hand, the propeller and edgewise flutter modes are not affected by the tower height variation.

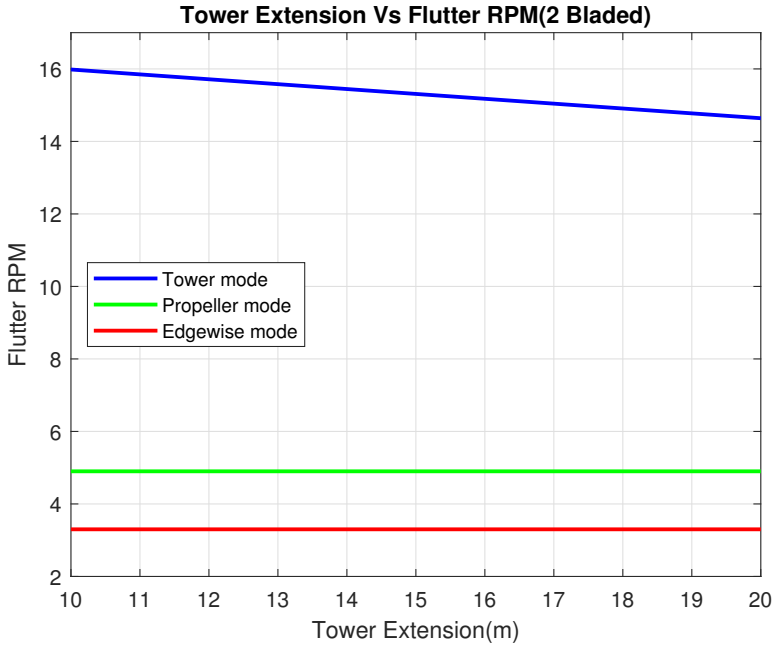

(a)

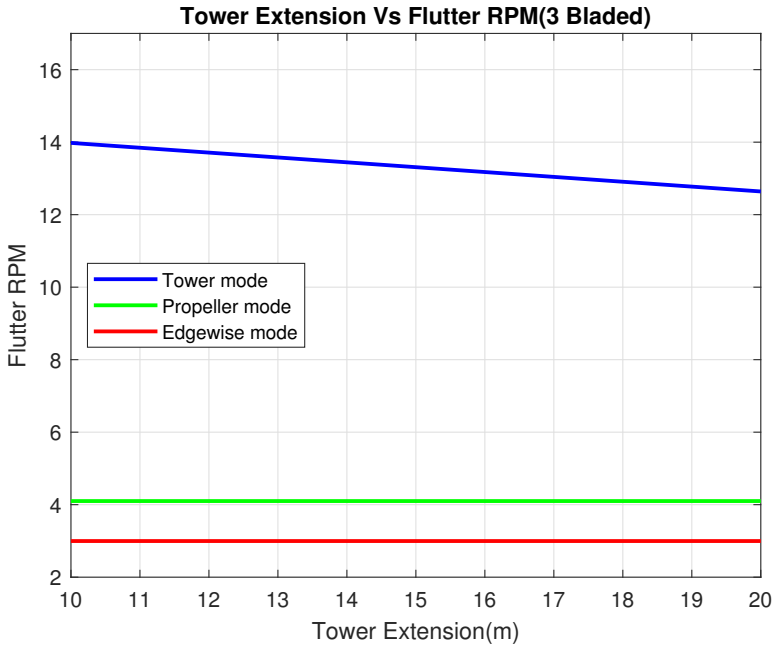

(b)

Figure 14: Tower Height Extension vs. Flutter RPM for (a) Two-Bladed and (b) Three-Bladed VAWT

5.2. Effect of Blade Chord Tapering on Modes and Flutter

As shown in Figure 15, four different blade chord tapering schemes were analyzed to observe their effects on the VAWT stability, which include (a) no taper (constant chord along span), (b) single taper at the bottom of the rotor, (c) single taper at the rotor top, and (d) double taper at both rotor top and bottom. For single taper bottom, the chord had maximum diameter at the root (bottom) i.e. the intersection of blade and tower, then the chord diameter was linearly decreased to 3 meters as the equator was approached,and after the equator till the other connection point between tower and blade ,the blade chord was kept fixed at 3 meters. The maximum chord size at the blade root were varied between 6 meters and 3 meters, while for each maximum chord size the linear descent to 3 meters towards the equator was considered as stated before. Similar pattern has been followed for tapering at the top of the blade with the difference being that in this case the maximum blade chord was at the blade top and tower intersection point, and subsequently the chord size was linearly reduced to 3 meters descending towards the blade equator. For the double tapered blade, maximum chord (ranging between 6 m to 3 meters) was considered at each blade and tower connection points, and then was linearly reduced down to 3 meters from each direction towards the blade chord. The no taper case implemented constant chord size ranging between 6 meters to 3 meters along the entire blade.

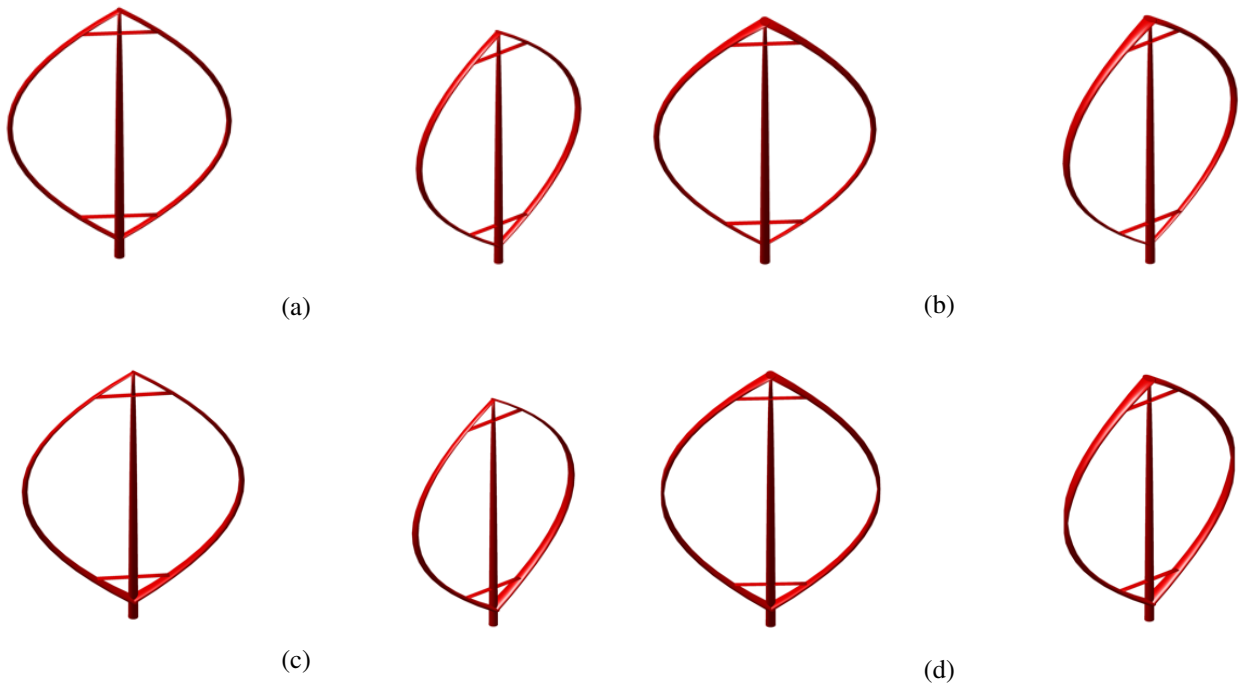

Figure 15: (a) No taper, (b) Single taper Top, (c) Single taper Bottom, (d) Double taper

We now study the critical flutter mode, the tower flutter mode, for these four blade chord tapering schemes, as presented in Figure 16. For tower mode flutter, although aerodynamics surrounding the blades changes with varying tapering scheme, it is observed that increasing the chord size increases the flutter RPM of the tower flutter mode for all types of tapering schemes since blade stiffness increases with larger chord sizes. Figure 16 indicates that the case where the blade has tapering only at the bottom (single taper bottom), from the blade root to the equator, is most suitable to delay the onset of flutter RPM, and that the case of single taper at the top is the worst in terms of flutter RPM. The concluding remark from this analysis is that lowering the center of gravity can help alleviate flutter concerns for the tower mode. The center of gravity varies with different tapering and chord sizes with the single bottom side [Figure 16(b)] tapering having the only decreasing trend in CG with increasing chord size.

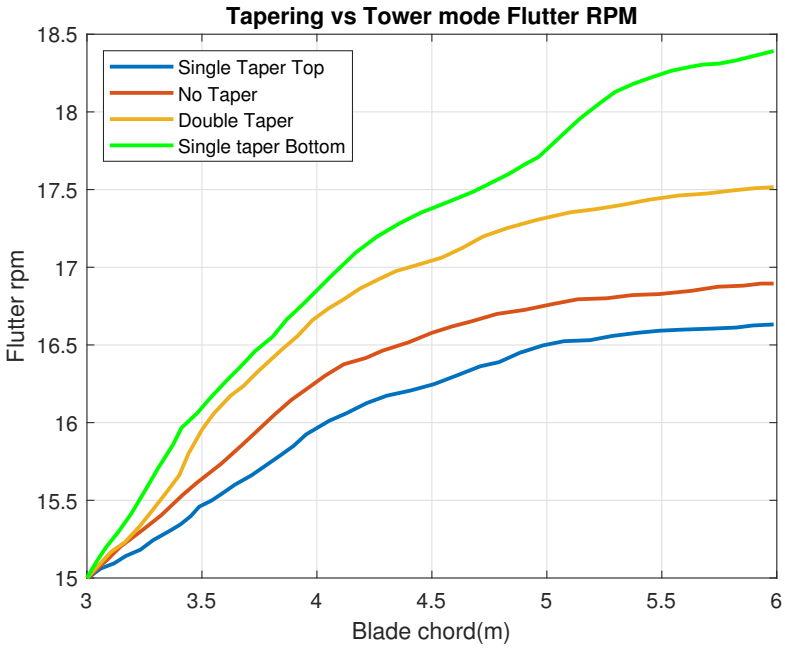

(a)

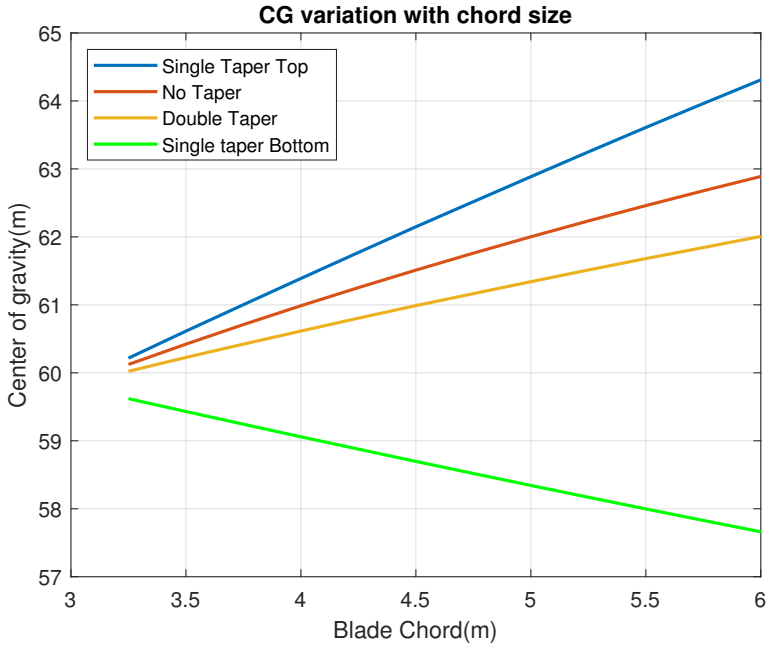

(b)

Figure 16: (a) Variation of flutter RPM for four tapering schemes with increasing chord size, (b) Change of center of gravity with increasing chord size

5.3. Effect of the Floating Platform on Modes and Flutter

In this section, we study the impact of the floating system for the offshore floating VAWT by comparing with the case of a land-based VAWT. As we will show, the floating platform has a sig-

nificant effect on the tower modes of two- and three-bladed offshore VAWTs. Figure 17 illustrates the difference in the frequency behavior of land-based and offshore UTD 5MW VAWT over a range of RPM, for the three tower height extensions considered in Figure 13. It is encouraging that the in-plane and out-of-plane tower frequencies increase for all six cases (Figure 17) when they are placed on a floating platform. For a two-bladed VAWT, the critical per-rev excitation lines are 1P, 3P, 5P, and 7P [28] where encountering these excitation lines may cause resonance issues. It is observed from the figures that a floating platform delays the encounter of tower modes with these per-rev excitations leading to potential to eliminate or mostly eliminate the resonance issue in comparison to the land-based case. A similar conclusion can be drawn for a three-bladed offshore VAWT where the 2P, 4P, 5P, and 7P per-rev excitation lines are of primary concern for resonance [28]. The frequency increase can be attributed to the fact that when a floating platform is attached to the bottom of the tower, it behaves more similar to a free boundary condition, and the entire turbine configuration acts similar to a beam with both free-free ends, which has a higher flexible mode frequency compared to a cantilever beam (as is the case for the land-based VAWT). The difference between two- and three-bladed offshore VAWTs with regards to resonance issue is that a three-bladed VAWT has comparatively lower tower mode frequencies over the RPM range, which makes it more prone to encountering the per-rev excitation lines.

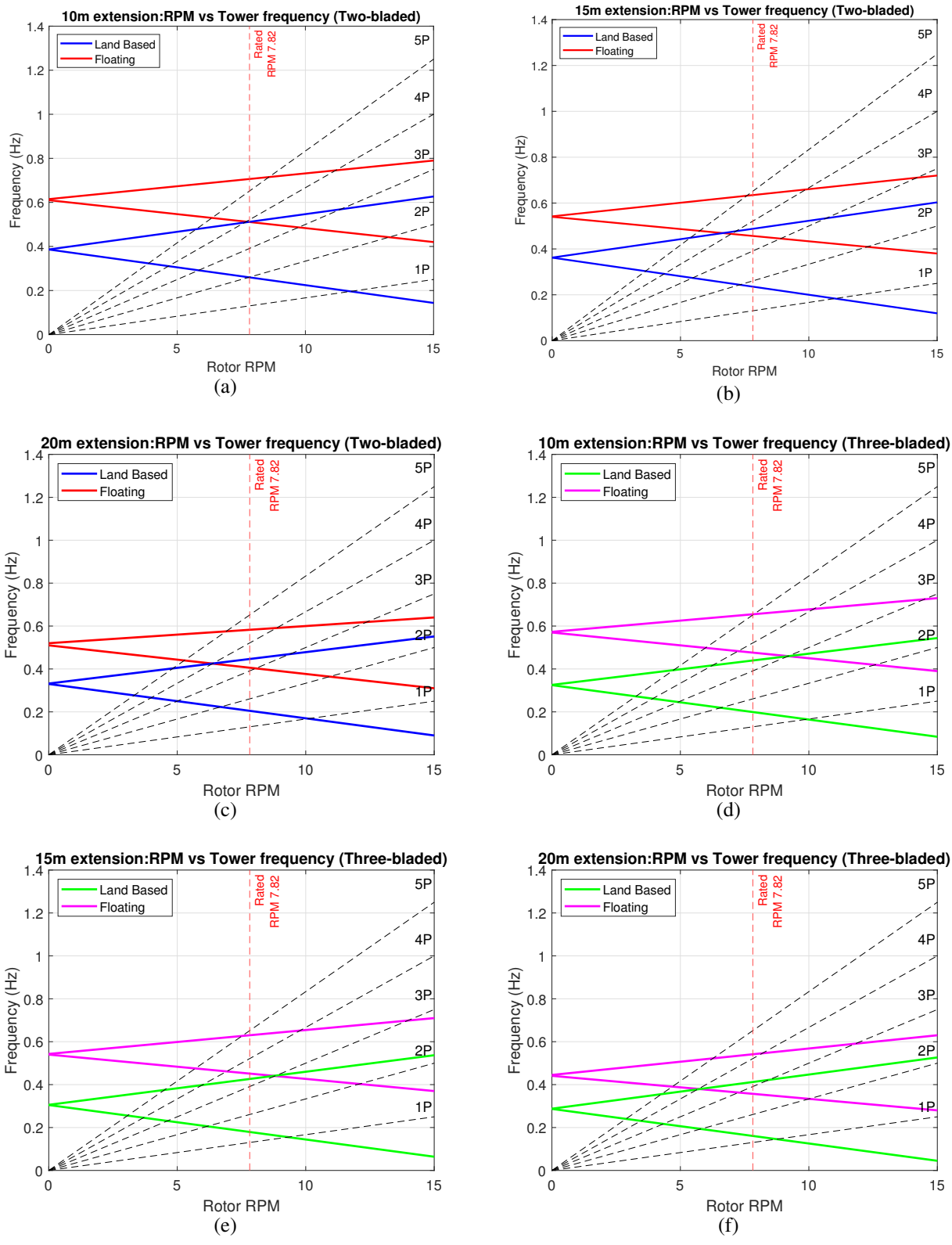

Figure 17: Effect of tower height on resonance of land-based and floating two-bladed (a-c) and three-bladed (d-f) VAWT

The preceding analysis examined only the impact of the floating platform on the tower mode;

however, for the floating system case rigid body modes (namely, the surge, sway, heave, roll, pitch and yaw modes) are introduced, which do not occur for the land-based case.

The method of adding the floating system model in OWENS has been validated against the commercial software OrcaFlex [33] based on the natural frequencies of the two-bladed floating VAWT. OrcaFlex is a commonly used tool for dynamic analysis of floating offshore systems. It can solve nonlinear dynamic mooring using a finite element method considering buoyancy, weight, viscous drag, hydrodynamic loads and so on.

The natural frequencies of the floating system in the six degrees of freedom were attained through free decay tests in OrcaFlex [25]. Comparison of the natural frequencies between OrcaFlex and the current study are summarized in Table 8. Compared to OrcaFlex, our study present lower frequencies with percent differences between 2.8% to 7.64%. These differences are mainly resulted from the different methods modeling the moorings between the two tools. As explained above, OrcaFlex applies a finite element method to account for all the loads acting on the moorings, while the floating system model in OWENS adopts a linear matrix to describe the mooring stiffness. Overall, the natural frequencies computed from OWENS agree with those from OrcaFlex with reasonable fidelity.

Mode	OrcaFlex (rad/s)	Current study (rad/s)	% Difference
Surge	0.17	0.15	-7.64
Sway	0.17	0.15	-7.64
Heave	3.53	3.39	-3.96
Roll	3.45	3.26	-5.5
Pitch	3.49	3.29	-5.73
Yaw	0.25	0.24	-2.8

Table 8: Comparison of natural frequencies of the two-bladed floating VAWT between OrcaFlex and OWENS

We perform an analysis of these rigid body vibration modes of the floating platform versus rotor RPM and present them in Figure 18. The trends in the six rigid body modes for the platform supported three-bladed VAWT are similar to the two-bladed design and hence are not separately discussed here. All the rigid mode frequencies except for the roll mode frequency remain relatively

constant the RPM range, as shown in Figure 18. The roll mode interacts with the rotating turbine initiating at about 8.5 RPM, where it starts to show a decaying trend. Although, as discussed before, the floating platform has the benefit of raising the tower mode frequencies resulting in less interaction with per-rev excitation frequencies, the presence of relatively lower rigid mode frequencies might raise concerns about potential resonance. For example, although the relatively higher heave, roll and pitch modes do not interact with per rev excitation lines within the operating RPM range, the other three lowest frequency rigid modes (surge, sway, and yaw) do have intersections with 1P and 2P excitation lines, thus it is recommended that these modes be examined for low RPM cases such as turbine start-up or shut-down for potential resonance by performing aero-elastic transient simulations.

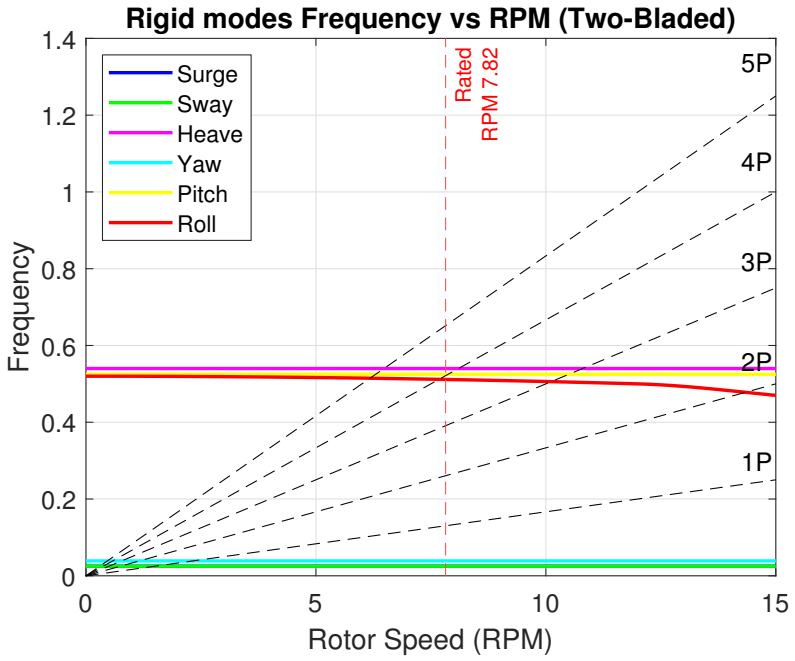

Figure 18: Floating VAWT rigid mode frequencies vs. RPM

We now turn our attention to investigate flutter for the floating VAWT system. Automated flutter analysis on the UTD 5MW VAWT has been performed using OWENS to examine the effect of a floating platform on the flutter instability. The result of the flutter analysis for the six lowest frequency flexible rotor modes is presented in Figure 19 as the damping versus RPM. Unstable flutter modes with negative damping have not been observed for the flexible rotor modes, thus Figure 19

shows that the turbine is not susceptible to flutter within the operating RPM range for these flexible rotor modes. However, the curves for the damping ratio of the tower, propeller, and edgewise modes start to flatten out at higher RPM, which may eventually cross the zero damping ratio line at higher RPM. Upon extending the analysis to higher speeds, it can be observed in Figure 20 that the tower mode, which was identified earlier as the critical flutter mode, goes unstable at about 44.2 RPM, which is much higher than the designed rotor operating RPM of 7.81. This delay in flutter speed can be attributed to the increased tower mode frequencies that result in placing the turbine on the floating platform as discussed earlier. As a result, the tower flutter RPM (for the UTD 5MW two-bladed VAWT) is increased by about 154% to 44.2 RPM on a floating platform versus 17.4 RPM for the land-based case. This is a very significant increase in flutter speed with the only change being the placement of the turbine on a floating platform (tension leg platform in this case) versus placement on land.

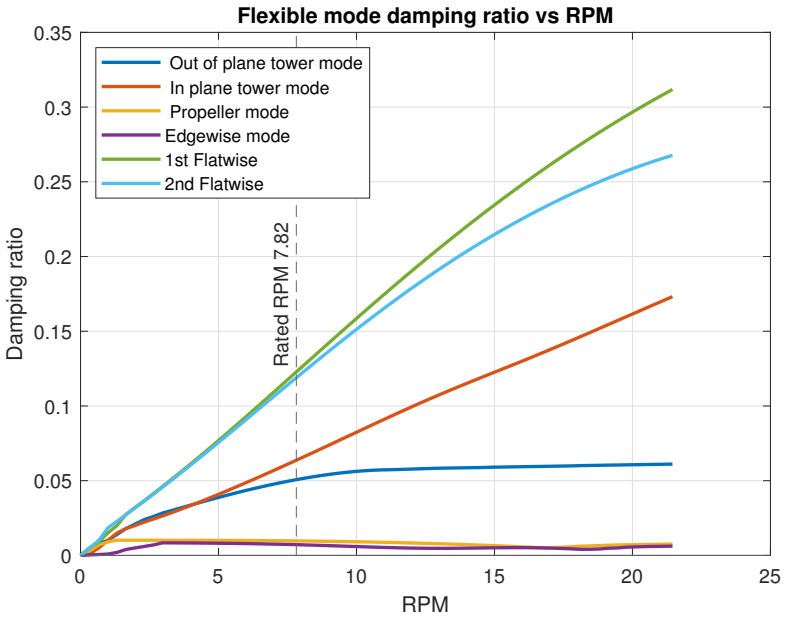

Figure 19: Flutter analysis of flexible modes (Damping ratio vs. RPM for two-bladed VAWT on floating platform)

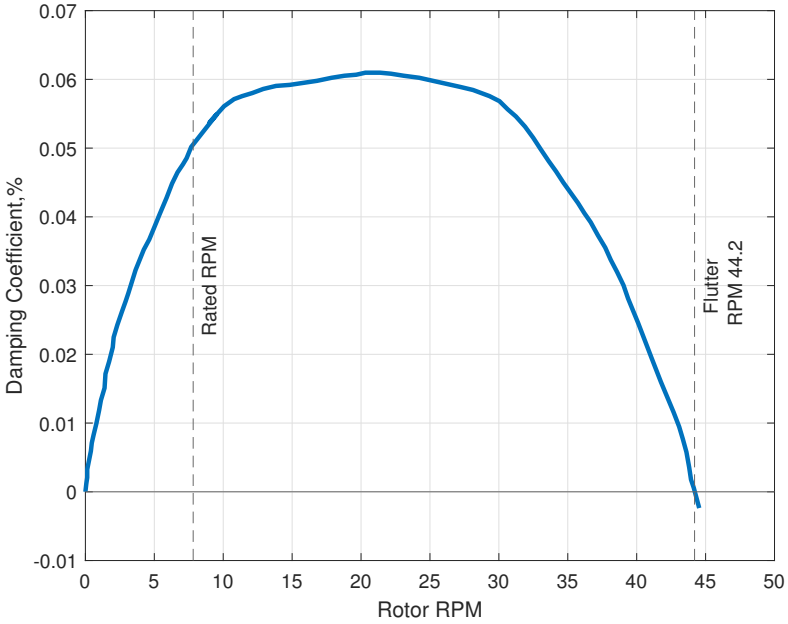

Figure 20: Tower mode damping ratio vs. RPM(For two-bladed VAWT on floating platform)

After analyzing the flexible modes, the flutter characteristics of the six rigid body modes (surge, sway, have, roll, pitch, and yaw modes) are also studied. Figure 21 shows the damping ratio of the rigid modes versus RPM. We find that the numerical values of the damping ratio for the rigid modes are two orders less than those for the flexible modes. The lowest damping can be observed in roll and pitch modes. These numerical values are comparable to the soft flutter mode values of the propeller and edgewise modes observed in the land-based VAWT.

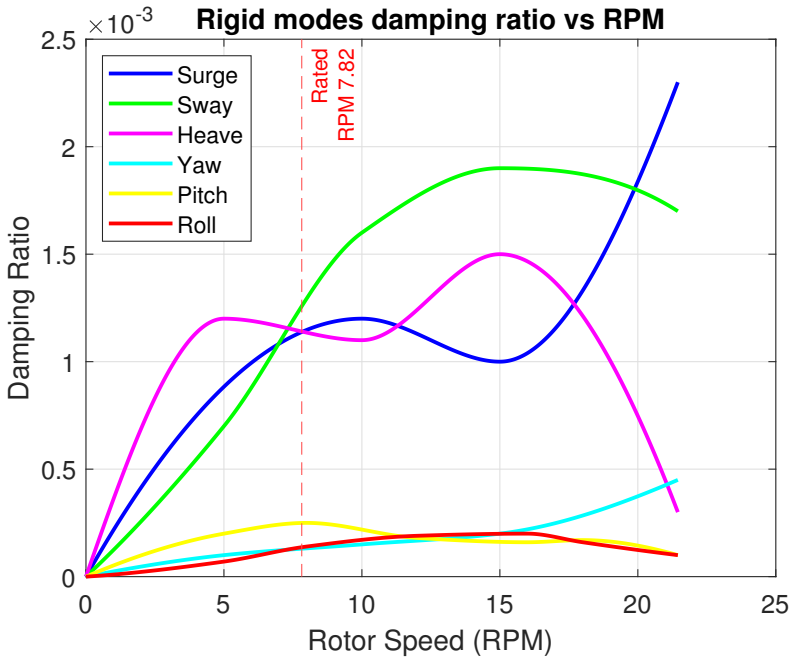

Figure 21: Flutter analysis of rigid modes (Damping ratio vs. RPM for two-bladed VAWT on floating platform)

Further analysis on the rigid body modes shows (Figure 22) that the pitch mode starts showing flutter instability at 44.8 RPM which is significantly higher than the operating RPM, and hence is not a major design concern.

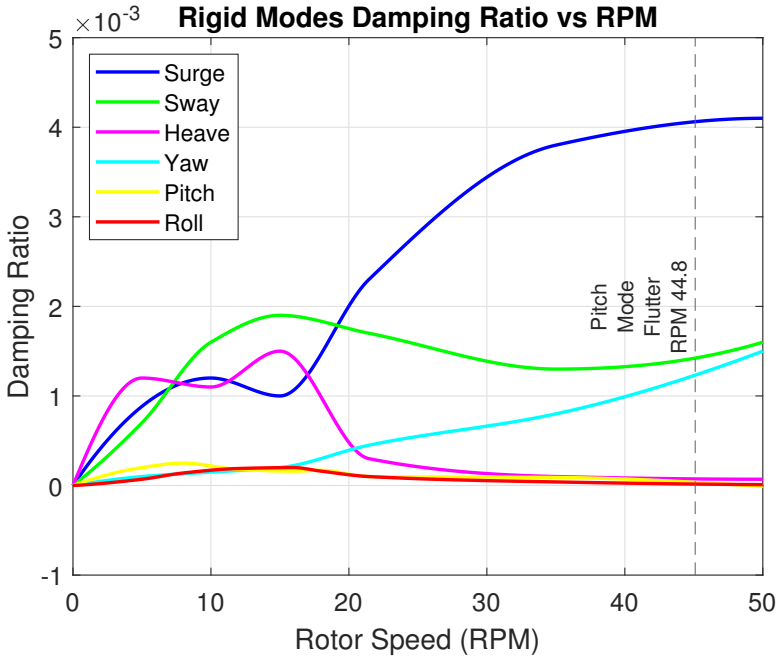

Figure 22: Flutter analysis of rigid modes (Damping ratio vs RPM for two-bladed VAWT on floating platform)

6. Conclusions

The benefits of large offshore wind farms have drawn significant research interest in recent years. Modal and flutter analysis of large-scale offshore VAWTs is crucial in safe operation over the lifespan of the turbine. The following are the major new contributions of this paper for modal and flutter analysis of offshore VAWT:

- Development of a coupled rotor-floating system model by adding the floating system in the OWENS code,
- Identification of dominant flutter mode characteristics of VAWT,
- Analysis of the effect of tower height and impact of number of blades on VAWT flutter RPM,
- Demonstration of the effect of blade tapering on VAWT flutter RPM, and
- Identification of flutter potential and characteristics of flexible and rigid modes of an offshore VAWT on a floating platform.

The focus of this study is analyzing the effect of tower height, blade numbers, blade tapering on the structural dynamics of VAWTs, and also developing a coupled structural dynamic model for modal and flutter analysis a floating VAWT by combining a rotor structural dynamics model (based on OWENS toolkit) with a linearized structural dynamics model for the floating system (hull and mooring). To ensure the accuracy of proposed model, a validation was conducted for both modal and flutter predictions with prior studies published for the Sandia 2-meter and Sandia 34-meter VAWTs. The results demonstrate an excellent agreement for predicting both the modes versus rotor speed and flutter RPM prediction.

Evaluating the flutter potential is crucial in designing lift generating structures, such as VAWTs. Past studies indicate that the classical flutter predictions in horizontal wind turbine blades exhibit flutter due to coupling of flapwise and torsional modes; however, the present results prove that distinctly different flutter characteristics are present for a VAWT as the tower mode is most unstable mode contributing to hard flutter instability for large-scale VAWTs. This is postulated to result from low damping that is inherent in the out-of-plane tower bending model. In order to further explore design space sensitivities, the effects of tower height on tower mode, propeller mode, and edgewise mode was studied for three cases of tower extension. It was found that tower height extension has a

neutral effect on the propeller and edgewise flutter mode but it has an significant, adverse impact on tower flutter mode.

Further, four blade-tapering schemes have been analyzed to understand which tapering is more effective in mitigating the flutter concern of VAWTs. All four tapering schemes showed potential to increase the flutter rpm with increasing chord sizes since larger chords stiffen the structure and increase the damping ratio for both two- and three-bladed turbines.

A technique to model a rigid floating platform support at the bottom of a flexible VAWT is introduced. The floating platform was observed to have a positive effect of raising the tower mode frequencies by 49%-68% compared to the land-based VAWT. Analysis of flutter showed that the flutter speed of hard tower mode was increased by 154% and the flutter of rigid modes was estimated at 5.7 times the operating RPM when moving from land-based to a floating system, which is a major benefit to moving offshore on floating systems. However, per-rev crossings of the lowest frequency rigid body modes may be a concern at low RPM operation, such a turbine start-up or shutdown, and should be analyzed. This work focused on modal and flutter characteristics for a floating offshore VAWT. In future work, it is suggested to consider unsteady hydrodynamic loads for the floating system model in addition to unsteady aerodynamic loads for the rotor. In addition, experimental studies would be beneficial to demonstrate the benefits of increased tower mode frequency and increased flutter speeds when placing a VAWT on a floating platform, as presented in this work.

Acknowledgment

The research presented herein was funded by the US Department of Energy Advanced Research Projects Agency-Energy (ARPA-E) under the ATLANTIS program with project title “A Low-cost Floating Offshore Vertical Axis Wind System” with Award No. DE-AR0001179. Any opinions, findings, and conclusions or recommendations expressed in this material are those of the authors and do not necessarily reflect the views of ARPA-E. The authors are grateful for the support of the ARPA-E program and staff, and the project team. The authors also acknowledge with true pleasure the contributions of Shulong Yao for strucutural design,Mohammad Sadman Sakib for aero design and Dr. Mohammad Jafari for reviewing the manuscript.

References

[1] D. T. Griffith, M. Barone, J. Paquette, B. Owens, D. Bull, C. Simao-Ferriera, A. Goupee, M. Fowler, Design studies for deep-water floating offshore vertical axis wind turbines, Tech. Rep. SAND2018-7002, Sandia National Laboratories (2018.

[2] D. T. Griffith, J. Paquette, M. Barone, A. J. Goupee, M. J. Fowler, D. Bull, B. Owens, A study of rotor and platform design trade-offs for large-scale floating vertical axis wind turbines, in: Journal of Physics: Conference Series 753 102003, 2016.

[3] J. DEIGN, Floating offshore wind holds promise for vertical-axis turbines, `https://www.greentechmedia.com/articles/read/floating-offshore-wind-holds-promise-for-vertical-axis-turbines` ((accessed Apr. 19, 2021)).

[4] B. L. Ennis, D. T. Griffith, System levelized cost of energy analysis for floating offshore vertical-axis wind turbines, Tech. Rep. SAND2018-9131, Sandia National Laboratories (2018).

[5] D. W. Lobitz, Aeroelastic stability predictions for a MW-sized blade, Wind Energy 7 (3) (2004) 211–224.

[6] M. H. Hansen, Aeroelastic instability problems for wind turbines, Wind Energy 10 (6) (2007) 551–577.

[7] D. T. Griffith, M. Chetan, Assessment of flutter prediction and trends in the design of large-scale wind turbine rotor blades, in: Journal of Physics: Conference Series 1037 042008, 2018.

[8] D. W. Lobitz, Dynamic analysis of darrieus vertical axis wind turbine rotors, in: 2nd DOE/NASA Wind Turbine Dyn. Workshop, 1981.

[9] W. N. Sullivan, Structural dynamic response characteristics of Darrieus vertical axis wind turbines, Tech. Rep. N-8315932, Sandia National Laboratories (1981).

[10] D. Popelka, Aeroelastic stability analysis of a Darrieus wind turbine, Tech. Rep. SAND82-0672, Sandia National Laboratories (1982).

[11] T. G. Carne, D. W. Lobitz, A. R. Nord, R. A. Watson, Finite element analysis and modal testing of a rotating wind turbine, in: 23rd Structures, Structural Dynamics and Materials Conference, 1982.

[12] D. W. Lobitz, T. D. Ashwill, Aeroelastic effects in the structural dynamic analysis of vertical axis wind turbines, 1986.

[13] D. T. Griffith, R. L. Mayes, P. S. Hunter, Excitation methods for a 60 kW vertical axis wind turbine, in: IMAC-XXVIII, 2010.

[14] F. Otterno, H. Bernhoff, Resonances and aerodynamic damping of a vertical axis wind turbine, Wind Engineering 36 (3) (2012).

[15] J. F. Kusnick, D. Adams, Vertical axis wind turbine operational modal analysis in sheared wind flow, in: the 30th IMAC, A Conference on Structural Dynamics, 2012.

[16] R. E. Meyers, Stability analysis of multi-megawatt Darrieus type floating vertical axis wind turbines, Tech. Rep. DTU Wind Energy-M-0099, DTU Wind Energy (2016).

[17] H. A. Madsen, The Actuator Cylinder: A Flow Model for Vertical Axis Wind Turbines, Institute of Industrial Constructions and Energy Technology, 1982.

[18] N. Najafi, U. S. Paulsen, Operational modal analysis on a VAWT in a large wind tunnel using stereo vision technique, Energy 125 (2017) 405–416.

[19] D. J. Malcolm, On the structural response of two- and three-bladed vertical axis wind turbine, Wind Energy 23 (2) (2019) 129–147.

[20] B. C. Owens, D. T. Griffith, B. R. Resor, J. E. Hurtado, Impact of modeling approach on flutter predictions for very large wind turbine blade designs, in: AHS 69th Annual Forum, 2013.

[21] T. M. Kai Wang, M. O. L. Hansen, A method for modeling floating vertical axis wind turbine, in: Proceedings of the ASME 2013 32nd International Conference on Ocean, Offshore and Arctic Engineering, 2013.

[22] B. P. Hand, A. Cashman, A floating vertical axis wind turbine for a deep offshore application, in: Conference: The 32nd International Manufacturing ConferenceAt: Queens University Belfast, UK, 2015.

[23] M. Borg, M. Collu, A comparison on the dynamics of a floating vertical axis wind turbine on three different floating support structures, in: EERA DeepWind'2014, 11th Deep Sea Offshore Wind RD Conference, 2014.

[24] K. S. Christina Anagnostopoulou, Hiroshi Kagemoto, A. Mizuno, Concept design and dynamic analyses of a floating vertical-axis wind turbine: case study of power supply to offshore greek islands, in: Journal of Ocean Engineering and Marine Energy volume 2,563 pages 85–104, 2016.

[25] Ju Gao, D. Todd Griffith, Mohammad Sadman Sakib, SungYoun Boo, A semi-coupled aero-servo-hydro numerical model for floating vertical axis wind turbines operating on tlps, in: Renewable Energy, Volume 181, 2021, 2021.

[26] B. C. Owens, Theoretical developments and practical aspects of dynamic systems in wind energy applications, Ph.D. thesis, Texas A&M University (2013).

[27] B. C. Owens, D. T. Griffith, Aeroelastic stability investigations for large-scale vertical axis wind turbines, in: The Science of Making Torque from Wind, 2014.

[28] B. C. Owens, D. T. Griffith, J. E. Hurtado, Modal dynamics and stability of large multi-megawatt deepwater offshore vertical-axis wind turbines: Initial support structure and rotor design impact studies, in: AIAA SciTech, 2014.

[29] Numad,in:https://energy.sandia.gov/programs/renewable-energy/wind-power/rotor-innovation/numerical-manufacturing-and-design-tool-numad.

[30] M. S. Sakib, D. T. Griffith, Parked and operating loads analysis in the aerodynamic design of multi-megawatt-scale floating vertical axis wind turbines, in: Wind Energ. Sci, 2021.

589 [31] S. Y. Boo, S. A. Shelley, D. Kim, A TLP floating foundation design with novel tendon mooring
590 technology for Hawaii offshore wind, in: 29th ISOPE Conference, 2019.

591 [32] S. Y. Boo, S. A. Shelley, D. Kim, Concept design of floating wind platforms of Y-wind and
592 T-wind for south east offshore of Korea, in: Korea Wind Energy Association, Fall Conference,
593 2018.

594 [33] Orcaflex, in: https://www.orcina.com/orcaflex.